Improving Economic Efficiency of Heat Pump Integration Into Distillation Columns of Process Plants Applying Different Pressures of Evaporators and Condensers

Stanislav Boldyryev *, Mariia Ilchenko , Goran Krajačić

Posted Date: 5 February 2024

doi: 10.20944/preprints202402.0217.v1

Keywords: process integration; heat pump; heat exchangers; industry electrification; energy saving; emission reduction; economic assessment.

Article

Improving Economic Efficiency of Heat Pump Integration into Distillation Columns of Process Plants Applying Different Pressures of Evaporators and Condensers

Stanislav Boldyryev [1,*], Mariia Ilchenko [2] and Goran Krajačić [1]

[1] Faculty of Mechanical Engineering and Naval Architecture, The University of Zagreb, Zagreb, Croatia; stanislav.boldyryev@fsb.hr
[2] National Technical University "Kharkiv Polytechnic Institute", Kharkiv, Ukraine; Mariia.Ilchenko@khpi.edu.ua
* Correspondence: stanislav.boldyryev@fsb.hr

Abstract: The electrification of process industries is one of the main challenges when building a low-carbon society since they consume huge amounts of fossil fuel generating different emissions. Heat pumps are one of the instruments to perform industrial sector of carbon-neutral market players. This paper proposes an approach to improve the economic feasibility of heat pumps within the process plants. Initial energy targeting with Grand Composite Curves was used and supplemented with the detailed design of the evaporator and compressor for different condensation and evaporation pressures. The trade-off between the capital cost of the heat pump and the electricity cost was investigated and optimal configurations were selected. The case study investigates the gas fractioning unit of a polymer plant where three heat pumps were integrated into distillation columns. The results demonstrated that the heat recovery is 174 MW and requires an additional 37.9 MW of electricity to reduce hot utility by 212 MW. The selection of evaporation and condensation pressure of heat pumps allows saving of 21.5 M€/y for 7 years of plant operation.

Keywords: process integration; heat pump; heat exchangers; industry electrification; energy saving; emission reduction; economic assessment

1. Introduction

The use of energy-saving technologies plays an important role in sustainable development and reducing environmental impact. One such technology that has become widely used is heat pumps.

A heat pump (HP) makes it possible to use low-potential heat sources and convert them into high-potential heat that can be used in production processes and the integration of renewable energies [1]. Heat pumps can be configured for different conditions and production requirements, making them the ideal choice for a variety of industries.

The use of heat pumps plays an important role in achieving energy efficiency, reducing the use of fossil energy resources, reducing negative emissions and protecting the environment. This enables industrial companies to reduce their ecological footprint, improve market competitiveness and contribute to sustainable development.

Heat pumps are used extensively in a variety of industries – primarily in the chemical, processing and food industries. The design strategy for or heat pump-assisted distillation system were proposed many yeas ago [2] but its importance inceased recently when environmental issue became a hot topic. Paper [3] investigates the recovery and upgrading of low-potential heat sources using HP (to generate useful process heat) and low-temperature heat engines (to generate electricity). The relevance and impact of wet compression on the performance of the HP are considered. In [4] a comparison of the parameter of specific energy consumption of heat pump dryers, combustion heated dryers and electrically heated dryers is made. In work [5] on an example of a dairy plant the application of the high-temperature HP is studied and a comparative assessment of reduction of CO_2

 doi:10.20944/preprints202402.0217.v1

emissions from heat pumps and boilers operating on natural gas is given. Similarly, in [6] for a dairy farm, a comparison is made of the heat pump water-heater (ASHPWH) system with other options: natural gas boiler, electric, liquefied petroleum gas (LPG) instant water heater, a solar water heater with an electric or natural gas backup.

The case study for the brewing process [7] considers an HP system with two parallel heat sources at different temperatures and times. Analysis of the proposed HP system shows that the CO_2 production from the consumption of electrical energy is reduced by 60%.

The use of HP is also widespread in the agricultural sector. Works [8–10] analysed the application of different types of TH for greenhouse heating, heating water used for watering and hot technical water preparation, including the assessment of technical aspects and cost-effectiveness of implementation. Heat pumps can also be used for district cooling of the residential sector during the summer by the use of existing district heat systems [11]. The authors [12] consider the energy, exergic, exergoeconomic and exergo-environmental analysis of an underfloor heating system integrated with the geothermal HP. Here, the distribution of losses in the system over the elements of the system separately is investigated, and the equivalent CO_2 emissions of heating a greenhouse with natural gas and an HP system are compared. In [13], the possibility of designing and building a coupled geothermal HP is confirmed. Based on the results of the assessment of the energy potential of the solar and geothermal sources, the energy balance in the greenhouse is calculated to determine the parameters of the geothermal HP using the vapor compression cycle.

Using the coal-fired power plant as an example, Zhang et al. [14] considered a cogeneration system based on an organic Rankine cycle (ORC) and absorption heat pump (AHP) to improve power output and heating capacity. The efficiency analysis shows that this cogeneration system can increase the power output and heating capacity of the plant. Cao et al. [15] compared the efficiency of different high-temperature HP systems to recover the heat from wastewater from the oil field and produce hot water. The analysis of the data obtained on system energy consumption and efficiency provides recommendations for the selection of a suitable heat recovery system with high heat output for industrial applications.

Another example of the application of an open absorption heat pump (OAHP) system combined with flash evaporation for coal-fired flue gas is the work of Zhang et al. [16]. An exergy analysis of the proposed schemes showed an improvement in the exergy efficiency of the optimized systems.

Su et al. [17] performed thermodynamic modelling and performance evaluation of a heat pump dryer by combining liquid desiccant dehumidification and mechanical vapour recompression. The comparison of the working principles and the performance of the proposed system and the reference system showed that the proposed scheme improves the energy efficiency of the heat pump drying system.

The potential for using an HP with CO2 as a working medium for the apple drying process was considered in [18]. An analysis of the system simulation results showed that the use of a closed-loop system is effective, but also leads to an increased drying time.

In the oil and chemical industry, it is common to use traditional distillation systems to separate mixtures of liquids. However, this process requires considerable use of fossil fuels as a heat source.

Waheed et al. [19] looked at a de-ethanisation unit of a Nigerian refinery as an example and enhanced the vapour recompression heat pump (VRHP) models that were developed to reduce heat loss and heat pump size. These strategies are based on reducing the heat differential across the heat pump by utilizing the process stream within the system, the external process stream and the utility streams.

For the production of n-butyl acetate and isopropyl alcohol, Liu et al. [20] proposed the heat pump-assisted dividing wall column for a reactive distillation system and a heterogeneous azeotropic distillation system. HP-assisted dividing wall columns are beneficial for cases where clean and highly effective electricity generation technologies are adopted and long-term profitability is considered.

 doi:10.20944/preprints202402.0217.v1

Long et al. [21] proposed an energy-efficient sequence for the natural gas liquid fractionation process. A hybrid system with a side reboiler and heat pump-assisted was proposed to maximize energy efficiency.

Long et al. [22] considered different HP configurations to improve the energy efficiency of distillation columns for separating R-410A and R-22. Top vapour superheating was proposed for improving the performance of the HP configuration, as well as for protecting the compressor from liquid leakage. The possibility of replacing the throttle valve with a hydraulic turbine, which would reduce the operating costs, is being considered.

Zhu et al. [23] analyzed the separation process of cyclohexane/sec-butyl alcohol/water azeotropic mixture by extractive distillation. The distillation process is optimized based on a sequential and iterative optimization algorithm. For further energy savings, several energy-optimized processes are proposed: the thermally coupled extractive distillation process(TCED), heat pump extractive distillation process (HPED), and heat pump combined with thermal coupling extractive distillation process (HPCWTCED).

Šulgan et al. [24] reviewed the production of ethyl acetate using an HP and presented a multi-objective evaluation based on energy requirements, economic analysis and safety analysis. As a result, the use of TH is highly recommended in both the conventional process and reactive column with a separation unit. Since a higher level of process integration is achieved with an HP, economic aspects are improved but at the same time, the safety aspects are worsened.

The application of HP in the distillation process may be the solution for process electrification. The case study in [25] analysed the natural gas liquid processing and assessed electrified thermal utility. The targeting for appropriate HP placement resulted in increased heat recovery and a reduction of energy cost by up to 41 %.

Florian Schlosser et al. [26] have reviewed HP and identified concepts for their integration across industries and processes based on the Grand Composite Curve (GCC) and demonstrated the savings potential. Kim et al. [27] proposed an optimal heat exchange network (HEN) with HP in a wastewater heat recovery system in the textile industry. The authors considered a two-step approach to design a heat exchange network and made an economic evaluation to minimise costs and maximise energy efficiency.

Case studies [28] and [29] of a milk spray dryer case study focused on the modelling and optimization an HP for convective dryers considering Pinch design principles. Different schemes for the integration of the drying process were considered, as well as the optimization of the operating parameters for maximum efficiency. Lincoln et al. [30] presented a fully electric milk evaporation system developed through an effective Process Integration and Electrification design method. A sensitivity analysis of the final process design was conducted, which showed that it applied to a wide range of operating conditions. The authors of [31] proposed a Pinch-based Total Site Heat Integration (TSHI) method, which is used for multi-level heat pump integration options at a meat processing site. The results of the Total Site approach in coke-to-chemicals demonstrated the appropriate placement of HP within inter-plant integration and showed a fast payback of 1.04 years [32].

In [33], several levels of heat integration were considered to reduce the energy consumption of a bioethanol plant. When the external energy demand and total annual cost of the different configurations, the authors concluded that the application of a heat pump is not recommended because of its high investment cost.

Paper [34] investigates the technical and economic performance of high-temperature heat pumps for use in the U.S. dairy industry. A model was created to estimate the coefficient of performance (COP), internal rate of return (IRR), net present value (NPV), and payback period (PBP). Capital costs, operations and maintenance (O&M) costs, heat pump lifetime, electricity prices, natural gas prices, and the cost of carbon were varied to conduct a parametric study of the factors affecting the break-even price of high-temperature HPs.

The authors [35] investigated a high-temperature cascade HP system using low-potential heat from wastewater to produce steam for industrial processes, developing a mathematical model of the system to analyze thermodynamic performance and economic efficiency.

 doi:10.20944/preprints202402.0217.v1

Paper [36] combines thermo-economic optimization with a solar thermal-assisted heat pump and a storage system. Here, two case studies are considered as examples: a dairy industry and a 2G bioethanol plant. A thermal and economic evaluation of the system was carried out to the supply of the heat load at the temperature level required at the required process temperature under different conditions and operating temperatures in the evaporator. Based on the established thermodynamic states the operating conditions of each HP component have been determined.

The authors of [37], [38] and [39] investigate the use of different types of refrigerants by comparing the performance of HP systems in terms of economics: total cost rate, investment and operating costs, capital costs of equipment, cost of CO2 penalty, energy and exergy efficiency, and NPV. The authors [40] consider a wet compression–resorption heat pump (CRHP) which operates NH3-H2O and NH3-CO2-H2O systems. The simple pay-back period for replacing an existing boiler with a CRHP system is calculated, depending on gas and electricity prices forecasted, the total investment costs, the installation costs, the annual fuel consumption costs, the operation and maintenance costs, the capital return coefficient. In paper [41] the integration of high temperature HP into a trigeneration system is proposed and analyzed. An exergy analysis was carried out to compare the proposed energy system with the traditional one (separate production, cogeneration, trigeneration). The economic evaluation has been analyzed using the methodology of the present value of electricity.

Papers [42] and [43] consider the thermodynamic and economic possibilities of using high-temperature and steam-generating HP in pulp and paper, textile, and automotive industries. The costs of consumption, investment, heat and maintenance are compared, taking into account the energy price and interest rate. In [44] a capacity-regulated HTHP system using a twin-screw compressor for waste heat recovery is proposed. Here, an economic comparison is made between the HTHP system and steam heating: thermal power of energy consumption, unit price, operating costs, capital costs, savings percentage, and payback period.

The authors of [45] and [46] evaluated the technical and economic feasibility of producing energy, steam and regenerative low-potential heat energy using mechanical vapour compression (MVC) heat pumps and absorption heat pumps, respectively. The authors [47] present an extensive economic analysis and environmental impact assessment of Heat Pump-Assisted Distillation under different conditions and scenarios: feed composition, plant capacity, and fuel price. Capital and operating costs, percentage of energy savings, payback period, total annual costs, and sensitivity analysis was performed.

In [48] optimization of tobacco drying HP recovering waste heat from monocrystal silicon furnace was considered. The issue is analyzed from the energy and economic side, investigating the influence of the heat exchange area on the system performance. A thermo-economic and economic model of the system is developed and experimentally verified.

The analysis underlines the prospective application of HP in industrial production belonging to different branches. Thus it is shown, that the majority of researchers are interested in the conjugate decision of questions of increase of efficiency of work of thermal installations and achievement of ecological stability. In terms of their performance heat pumps markedly exceed almost all other available technologies, and the feasibility of their application is confirmed by technical and economic calculations by comparing many parameters.

This work analyses the application of HP within the industrial processes updating the tageting procedure by GCC. Different condensation and evaporation pressures of HP are used for the detailed design of HP heat exchangers. The trade-off between energy cost and capital cost for obtaining a detailed configuration of heat pumps was analysed and the best economic solution was selected. It is applied for the gas fractioning process of the polymer plant where 3 heat pumps were analysed utilising the waste heat of distillation column condensers to column reboilers. The results of the case study provided the background for the discussion on the author's hypothesis of the improvement of the economic feasibility of the HP application.

 doi:10.20944/preprints202402.0217.v1

The remaining part of the paper gives the framework and method description (Section 2), followed by case studies of the gas fractioning process of polymer plant (Section 3), a discussion of the results in Section 4 and conclusions.

2. Materials and Methods

The method proposed in the current paper is based on the scientific hypothesis that there is a trade-off between energy and capital costs when applying the heat pump in industrial processes. The application of the heat pumps in distillation columns is more complex due to phase changes of the heat carriers on both sides of the heat exchanger. The reduced capital costs, energy costs and total annual cost of heat pumps are analyzed for different condensation and evaporation temperature/pressure of refrigerant.

The algorithm treating the proposed methodology is following:

1. Definition of the process streams that should be heated and cooled by heat pump with the use of the GCC (Figure 1).
2. Placement of the heat pump and set the initial energy targets for both thermal energy and power specifying the current ΔT_{min} between process and utility (refrigerant).
3. Simulation of the Heat Pump in Aspen HYSYS [49] environment under the pressure acceptable drop of the condenser and reboiler.
4. Based on the simulation results, the calculation of the detailed configurations and capital costs of the condenser and reboiler.
5. Calculation of the compressor capital cost.
6. Calculation of the annualized capital cost of the HP equipment using the cost factors.
7. Calculation of the total annualized cost (TAC).
8. Changing the refrigerant pressure in the compressor inlet/outlet and repetition of the previous steps.
9. Selection of the HP configuration with min TAC.
10. Perform a sensitivity analysis of the results by applying different electricity prices.

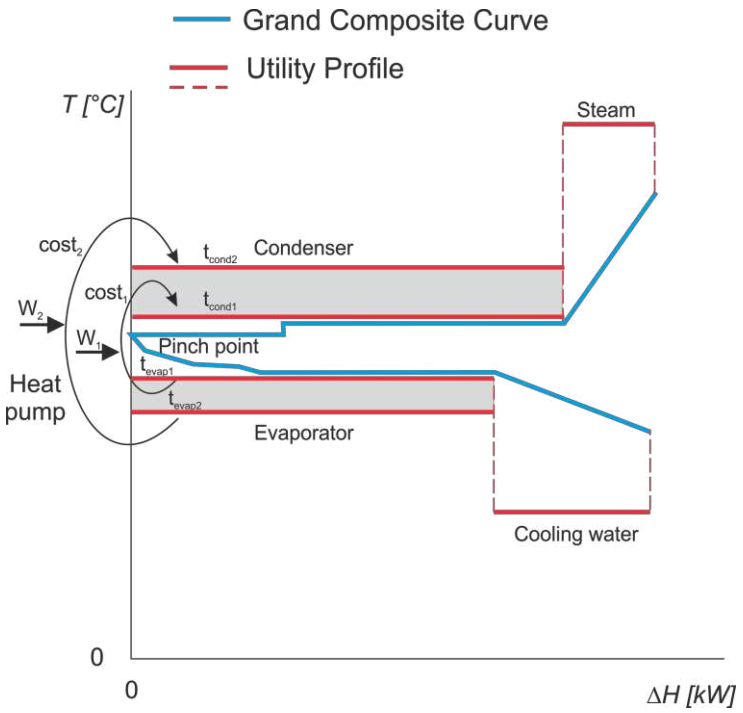

Figure 1. Different options for the HP integration within the industrial processes.

The algorithm is based on the following mathematical formulations.

Mass and heat balances are calculated from Equations 1 and 2.

 doi:10.20944/preprints202402.0217.v1

$$\sum_{j=1}^{J} M_j^{In} = \sum_{J=1}^{J} M_j^{Out} + M_{losses} \tag{1}$$

$$\sum_{j=1}^{J} \left(h_j^{In} M_j^{In}\right) + \sum_{i=1}^{I} W_i = \sum_{j=1}^{J} \left(h_j^{Out} M_j^{Out}\right) + Q_{losses} \tag{2}$$

Heat transfer area is defined for shell-and-tube heat exchangers from Equation (3):

$$Q = UA\Delta T_{LM} Ft \tag{3}$$

where Ft factor taken equal to 1 for full countercurrent and ΔT_{LM} defined from Equation (4):

$$\Delta T_{LM} = \frac{(T_{inH} - T_{outC}) - (T_{outH} - T_{inC})}{ln\frac{(T_{inH} - T_{outC})}{(T_{outH} - T_{inC})}} \tag{4}$$

The overall heat transfer coefficient is defined by the film for condensation outside of a horizontal tube with Kern correlations [50]:

$$h_C = 0.725\left(\frac{k_L^3 \rho_L^2 \Delta H_{VAP} g}{d_0 \mu_L \Delta T}\right)^{\frac{1}{4}} \tag{5}$$

and evaporation of kettle and horizontal thermosyphon reboilers is due to [51]

$$h_{NB} = 0.182 P_C^{0.67} q^{0.7} \left(\frac{P}{P_C}\right)^{0.17} \tag{6}$$

The detailed designs of the condenser/reboiler and its price were found with Aspen EDR Heat Exchanger software.

COP of HP is found from simulation results in Aspen HYSYS:

$$COP_{HP} = \frac{Q_{HP} + W}{W} \tag{7}$$

The capital cost of the compressor is defined capital cost of the compressor was estimated based on Chemical Engineering Indexes and Marshall and Swift by Equation (8):

$$CAPEX_{Comp} = 98{,}400\left(\frac{W}{250}\right)^{0.46} f(t) \cdot f(p) \cdot f(m) \tag{8}$$

where f(m) is the correction factor for materials of construction, f(p) is the correction factor for design pressure and f(t) is the correction factor for design temperature.

The annualized capital cost of the HP was obtained from condenser, evaporator and compressor cost using the fractional interest rate (FIR), loan period (NY) and Lang Factor (Lang). Lang Factor accounts for the cost of installation, piping, control system, insulation, engineering fees and other costs.

$$ACC = \left(CAPEX_{Comp} + CAPEX_{Cond} + CAPEX_{Evap}\right) \cdot Lang \cdot \left(\frac{\mathrm{FIR}(1 + \mathrm{FIR})^{\mathrm{NY}}}{(1 + \mathrm{FIR})^{\mathrm{NY}} - 1}\right) \tag{9}$$

Energy cost was found using the electricity target of HP and average electricity cost:

$$EC = W \cdot c_e \tag{10}$$

TAC was calculated based on capital cost and energy cost obtained from Equations 9 and 10.

$$TAC = ACC + EC \tag{11}$$

 doi:10.20944/preprints202402.0217.v1

3. The case study

3.1. Process description

The case study examines the streams of the gas fractioning unit of the polymer plant and integrates three heat pumps into the process to electrify the thermal utility for further use of renewable energies. This paper examines the operation of three heat pumps using Refrig-21 as a refrigerant.

HP-1. The refrigerant vapour flow with a temperature of 57.26 °C and a pressure of 480 kPa enters the compressor, where the refrigerant vapour is compressed to 900 kPa. From the compressor, the refrigerant with a temperature of 96.31 °C is directed to the condenser, where the refrigerant is cooled and condensed due to heat exchange with heat consumers (flow with a temperature of 79.97 °C and a pressure of 1011 kPa). The condensed liquid refrigerant with a temperature of 82.29 °C and a pressure of 895 kPa passes through the control valve, where the refrigerant is throttled. Next, the refrigerant with a temperature of 57.65 °C and a pressure of 485 kPa enters the evaporator. The refrigerant evaporates, giving off the heat of evaporation to cold consumers (flow with a temperature of 66.46 °C and a pressure of 907 kPa).

HP-2. The refrigerant vapour flow with a temperature of 52.37 °C and a pressure of 420 kPa enters the compressor, where the refrigerant vapour is compressed to 900 kPa. From the compressor, the refrigerant with a temperature of 99.30 °C is directed to the condenser, where the refrigerant is cooled and condensed due to heat exchange with heat consumers (flow with a temperature of 79.97 °C and a pressure of 1011 kPa). The condensed liquid refrigerant with a temperature of 82.29 °C and a pressure of 895 kPa passes through the control valve, where the refrigerant is throttled. Next, the refrigerant with a temperature of 52.80 °C and a pressure of 425 kPa enters the evaporator. The refrigerant evaporates, giving off the heat of evaporation to cold consumers (flow with a temperature of 57.35 °C and a pressure of 1911 kPa).

HP-3. The refrigerant vapour flow with a temperature of 45,94 °C and a pressure of 380 kPa enters the compressor, where the refrigerant vapour is compressed to 2000 kPa. From the compressor, the refrigerant with a temperature of 157.9 °C is directed to the condenser, where the refrigerant is cooled and condensed due to heat exchange with heat consumers (flow with a temperature of 99.06 °C and a pressure of 775 kPa). The condensed liquid refrigerant with a temperature of 120.8 °C and a pressure of 1995 kPa passes through the control valve, where the refrigerant is throttled. Next, the refrigerant with a temperature of 46.43 °C and a pressure of 355 kPa enters the evaporator. The refrigerant evaporates, giving off the heat of evaporation to cold consumers (flow with a temperature of 54.33 °C and a pressure of 1914 kPa).

The thermal and physical properties of all process streams were simulated in the UniSim environment. The simulation details of heat pumps are shown in Figure 2. The properties of process streams are shown in Table 1. The material and energy balances of heat pumps are presented in Table 3.

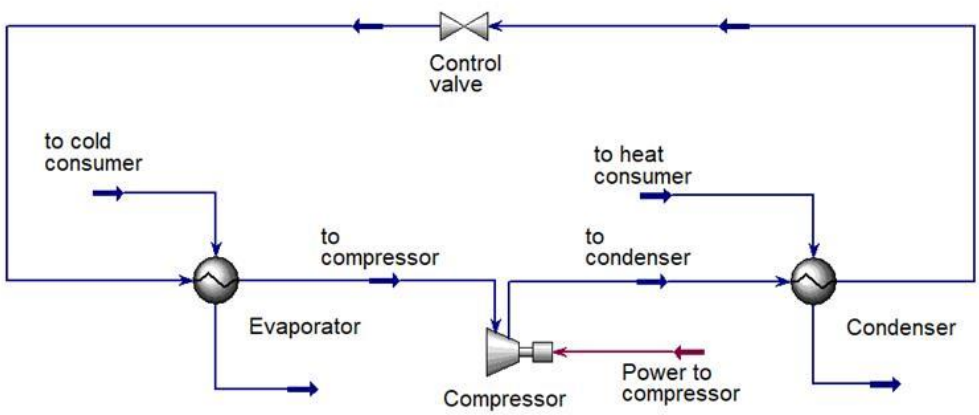

 doi:10.20944/preprints202402.0217.v1

Figure 2. PFD of heat pump simulated in UniSim Design..

Table 1. Composition of process streams.

Streams	Mass flow, kg/h	Component mass fractions						
		Ethane	Propane	i-Butane	n-Butane	i-Pentane	n-Pentane	Refrig-21
HP-1								
To condenser	1,867,979	–	–	–	–	–	–	1.0000
To cold consumer	1,146,672	–	0.0364	0.5551	0.4085	–	–	–
To heat consumer	1,297,954	–	–	–	0.9987	0.0013	–	–
HP-2								
To condenser	389,690	–	–	–	–	–	–	1.0000
To cold consumer	254,492	0.0159	0.9092	0.0718	0.0032	–	–	–
To heat consumer	272,854	–	–	–	0.9990	0.0010	–	–
HP-3								
To condenser	1,493,798	–	–	–	–	–	–	1.0000
To cold consumer	761,491	0.0116	0.9863	0.0021	–	–	–	–
To heat consumer	1,131,018	–	–	–	–	0.4105	0.3355	0.2540

Table 2. Parameters of the heat pump equipment.

Parameters	Evaporator			Condenser		
	HP-1	HP-2	HP-3	HP-1	HP-2	HP-3
Duty, kW	95,889	19,703	62,185	106,692	22,430	82,863
Tube side feed mass flow, kg/h	1,867,979	389,690	1,493,798	1,867,980	389,690	1,493,798,
Shell side feed mass flow, kg/h	1,146,672	254,492	761,491	1,297,954	272,854	1,131,018,
Tube inlet temperature, °C	57.65	52.80	45.44	97.07	99.30	138.12
Tube outlet temperature, °C	58.00	52.37	44.95	82.29	82.29	106.04
Shell inlet temperature, °C	66.46	57.35	54.35	79.97	79.97	99.06
Shell outlet temperature, °C	62.97	54.00	47.83	79.80	79.81	102.30
Tube inlet pressure, kPa	485	425	345	900	900	1,500
Tube outlet pressure, kPa	480	420	340	895	895	1,495
Shell inlet pressure, kPa	907	1900	1914	1,011	1,011	775
Shell outlet pressure, kPa	902	1,906	1,909	1,006	1,006	770
Compressor						
	HP-1	HP-2	HP-3			
Power, kW	10,804	2,727	20,678			
COP	9.88	8.22	4.01			

Table 3. Mass and Energy balance of heat pump.

Inlet streams			Outlet streams		
Stream name	Mass flow, kg/h	Energy flow, kW	Stream name	Mass flow, kg/h	Energy flow, kW
HP-1					

 doi:10.20944/preprints202402.0217.v1

To cold consumer	1,146,672	-704,091	To cold consumer	1,146,672	-799979
To heat consumer	1,297,954	-864,174	To heat consumer	1,297,954	-757482
Power to compressor		10,804			
		HP-2			
To cold consumer	254,492	-166,615	To cold consumer	254,492	-186,317
To heat consumer	272,854	-181,666	To heat consumer	272,854	-159,236
Power to compressor		2,727			
		HP-3			
To cold consumer	761,491	-500,131	To cold consumer	761,491	-562,317
To heat consumer	1,131,018	-772,202	To heat consumer	1,131,018	-689,339
Power to compressor		20,678			
Total flow	**4,864,481**	**-3,154,670**	**Total flow**	**4,864,481**	**-3,154,670**
			Imbalance	**0.00 %**	**-8.14 e-009 %**

3.2. Scenarios

3.2.1. Scenario 1: The influence of changes in pressure at the condenser inlet on the operating parameters of the HP at a constant pressure at the evaporator outlet is analyzed.

The temperature and pressure of the refrigerant flow at the outlet of the evaporator remain constant. An increase the flow pressure in the flow pressure at the inlet to the condenser led to an increase in the flow temperature after the condenser, an increase in the power consumption of the compressor and a decrease in the COP parameter. The results of Scenario 1 are presented in Table 4.

Table 4. Data for Scenario 1.

	HP-1		**HP-2**		**HP-3**	
	Start point	Endpoint	Start point	Endpoint	Start point	Endpoint
Evaporator						
Inlet pressure, kPa	480		420		340	
Evaporation temperature, °C	57.26		52.37		44.95	
Condenser						
Inlet pressure, kPa	900	1,300	900	1,300	1,500	1,900
Condensation temperature, °C	82.29	99.08	82.29	99.08	106.00	118.11
Compressor						
Power consumption, kW	10,808	17,934	2.727	4.234	20,678	25,020
COP	9.87	5.95	8.22	5.30	4.01	3.31

3.2.2. Scenario 2: The influence of changes in pressure at the evaporator outlet on the operating parameters of the HP at a constant pressure at the condenser inlet is analyzed.

 doi:10.20944/preprints202402.0217.v1

The pressure at the inlet of the condenser and the temperature of the refrigerant flow after the condenser remains constant. Reduction in the flow pressure at the outlet of the evaporator led to a decrease in the temperature of the refrigerant flow at the inlet of the compressor, an increase in the power consumption of the compressor and a decrease in the COP parameter. The results of Scenario 2 are presented in Table 5.

Table 5. Data for Scenario 2.

	HP-1		**HP-2**		**HP-3**	
	Start point	Endpoint	Start point	Endpoint	Start point	Endpoint
Evaporator						
Inlet pressure, kPa	480	101	420	120	340	101
Evaporation temperature, °C	57.26	9.55	52.37	13.13	44.95	8.53
Condenser						
Inlet pressure, kPa	900		900		1500	
Condensation temperature, °C	82.29		82.29		106.00	
Compressor						
Power consumption, kW	10,808	33,442	2,727	6,549	20,678	34,035
COP	9.87	3.19	8.22	3.43	4.01	2.44

3.2.3. Scenario 3: The influence of changes in pressure at the evaporator outlet and condenser inlet on the operating parameters of the HP is analyzed.

Simultaneous reduction of the flow pressure at the outlet of the evaporator and increase the flow pressure at the inlet of the condenser led to a decrease in the temperature of the refrigerant flow at the inlet of the compressor, increase in the temperature of the refrigerant flow after the condenser, increase in the power consumption of the compressor and a decrease in the COP parameter. The results of Scenario 3 are presented in Table 6.

Table 6. Data for Scenario 3.

	HP-1		**HP-2**		**HP-3**	
	Start point	Endpoint	Start point	Endpoint	Start point	Endpoint
Evaporator						
Inlet pressure, kPa	480	101	420	120	340	101
Evaporation temperature, °C	57.26	9.55	52.37	13.13	44.95	8.53
Condenser						
Inlet pressure, kPa	900	1,300	900	1,300	1,500	1,900
Condensation temperature, °C	82.29	99.08	82.29	99.08	106.00	118.11
Compressor						
Power consumption, kW	10,808	40,234	2,727	8,089	2,0678	38,502
COP	9.87	2.65	8.22	2.77	4.01	2.15

3.3. Variables and Constraints

 doi:10.20944/preprints202402.0217.v1

For the economic assessment of HP operation parameters, the following variables were used:

- Y = 8670 h;
- Lang = 4.72;
- FIR = 0.1;
- NY = 7 years;
- $c_{e\ min}$ = 0.12 EUR/kWh (minimal EU price), $c_{e\ avg}$ = 0.21 EUR/kWh (average EU price), $c_{e\ max}$ = 0.39 EUR/kWh (maximal EU price) [52];
- Condenser pressure;
- Evaporator pressure;
- Compressor power;
- COP;
- Heat transfer area of the condenser;
- Heat transfer area of the evaporator.

The next constraints were used:

- Minimum pressure at the compressor inlet 101.3 kPa;
- Maximum pressure at the compressor inlet of HP-1 480 kPa;
- Maximum pressure at the compressor inlet of HP-2 420 kPa;
- Maximum pressure at the compressor inlet of HP-3 380 kPa;
- Minimum pressure at the compressor outlet of HP-1 900 kPa;
- Minimum pressure at the compressor outlet of HP-2 900 kPa;
- Minimum pressure at the compressor outlet of HP-3 2000 kPa;
- The acceptable condenser pressure drops (tubes/shell) is 5 kPa;
- The acceptable evaporator pressure drop (tube/shell) is 5 kPa;
- Compressor efficiency (adiabatic) is 75 %;
- Heat exchanger type is shell-and-tube for both evaporator and condenser;
- Tube type is plain;
- The tube material is carbon steel.

The design and cost of the condenser and evaporator were selected using the Aspen Exchanger Design & Rating application. The next Aspen databases were used for capital cost assessment of condenser and evaporator [53]:

- D_FXPRIV.PDA Private properties chemical databank properties;
- D_IDPRIV.PDA Private properties chemical databank index;
- D_VAPRIV.PDA Private properties chemical databank properties;
- N_MTLDEF.PDA Default materials for generic materials (ASME);
- N_MTLDIN.PDA Default materials for generic materials (DIN);
- N_MTLCDP.PDA Default materials for generic materials (AFNOR);
- N_PARTNO.PDA Part number assignment for bill of materials;
- N_PRIVI.PDA Private properties materials databank index;
- N_PRIVP.PDA Private properties materials databank properties;
- N_STDLAB.PDA Fabrication standards, procedures, costs, etc.;
- N_STDMTL.PDA Fabrication standards as function of materials;
- N_STDOPR.PDA Fabrication operation efficiencies;
- N_STDWLD.PDA Fabrication welding standards;
- N_STDPRC.PDA Private materials prices.

 doi:10.20944/preprints202402.0217.v1

4. Results and discussion

4.1. Heat pump 1.

4.1.1. Average electricity price

The results of the TAC assessment of HP 1 for all three case studies are presented in Figure 1. The correlation of Scenario 1 has a minimum condenser pressure of 1,050 kPa and the overall trend has extremum. The correlation of Scenario 2 shows that TAC is increasing from the starting point of condensing pressure 480 kPa to the endpoint of 101.3 kPa. The TAC in Scenario 3 has also an increasing trend from the starting point to the end when both, condensation and evaporation pressure, are changed. The minimum TAC of all three case studies resulted in Scenario 1 and it is 33.26 M€.

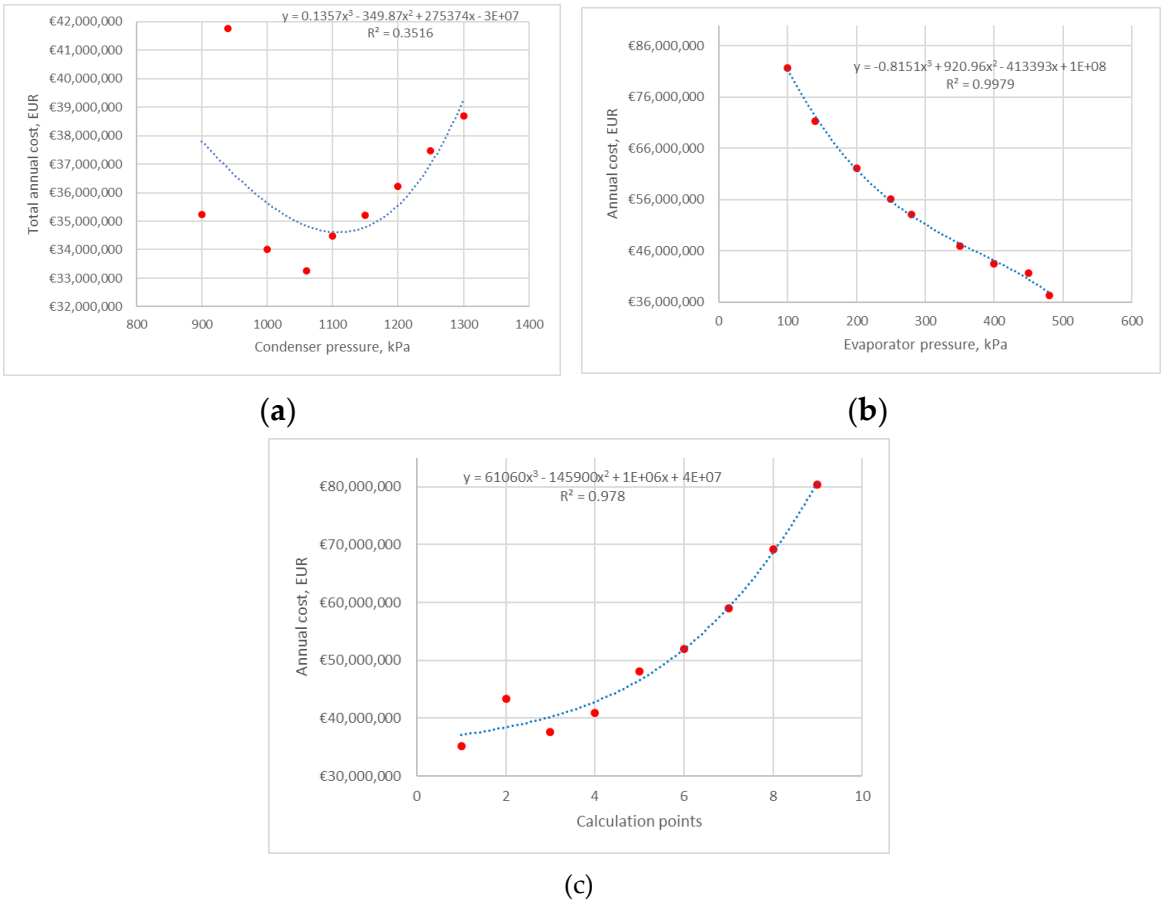

Figure 3. Total annual cost correlation of Heat Pump 1 for average electricity price: (**a**) scenario 1; (**b**) scenario 2; (**c**) scenario 3.

The capital cost distribution between compressor, evaporator and condenser is shown in Figure 4. In Scenario 1 (Figure 4a), the share of capital cost is shifting between the condenser and compressor, while the evaporator cost remains almost the same from calculation point 3. Minimum TAC is observed for calculation point 4 (Figure4a). Evaporator cost is dominated in Scenario 2 (Figure 4b) while decreasing the evaporation pressure. The share of the evaporator cost is between 62 and 72 %. The compressor cost in Scenario 3 (Figure 4c) is the highest in capital cost share and it is increasing due to COP reduction.

 doi:10.20944/preprints202402.0217.v1

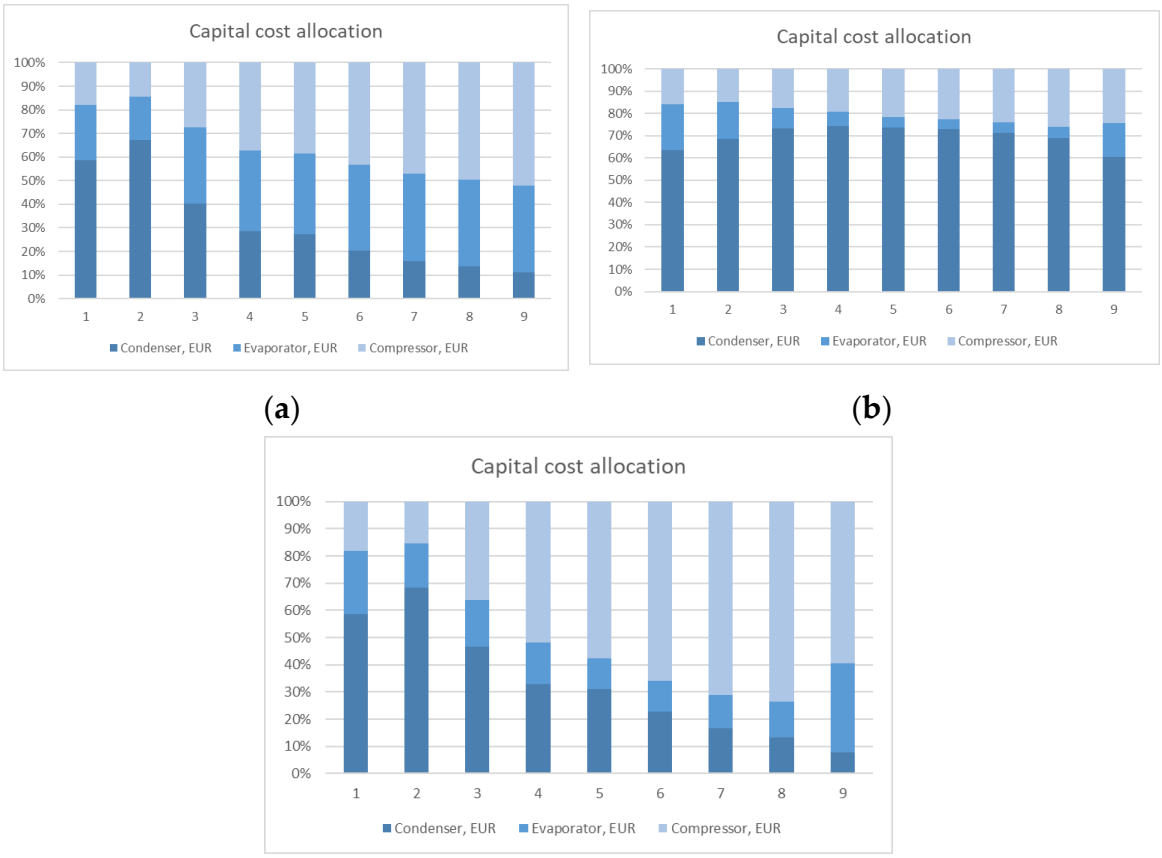

Figure 4. Capital cost allocation of Heat Pump 1: (**a**) scenario 1; (**b**) scenario 2; (**c**) scenario 3.

The total cost share is shown in Figure 5 and the energy cost is about 50 % for two calculation points, further, the decrease in COP energy cost is determinative. If the minimum TAC of heat pump 1, is shown in Figure 5a, point 4 and the share of energy cost is 72 %.

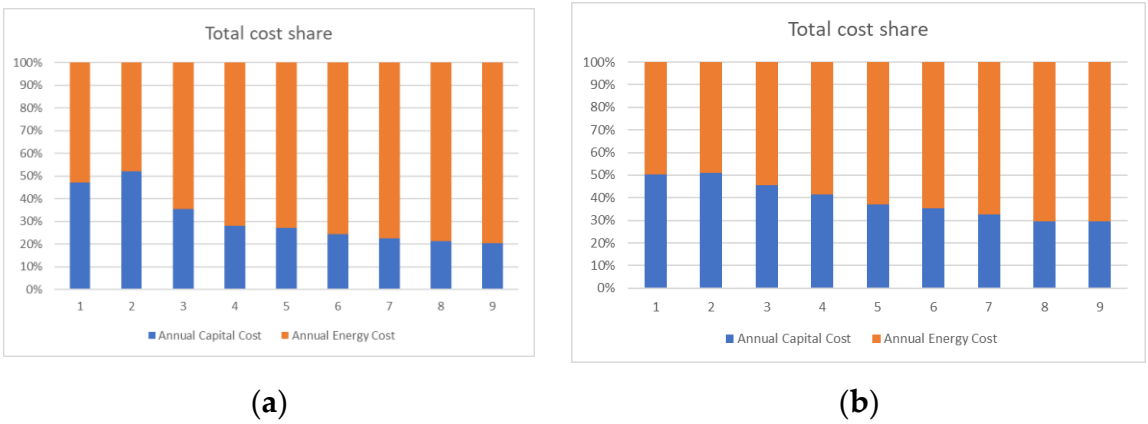

Preprints.org (www.preprints.org) | NOT PEER-REVIEWED | Posted: 5 February 2024 doi:10.20944/preprints202402.0217.v1

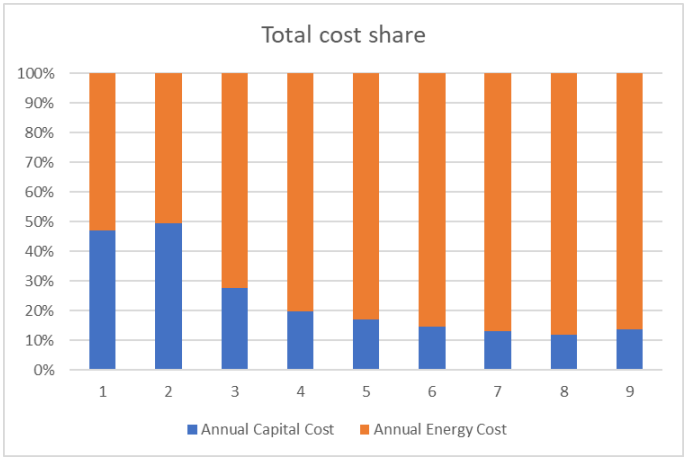

(c)

Figure 5. Total cost distribution of Heat Pump 1 for average electricity price: (**a**) scenario 1; (**b**) scenario 2; (**c**) scenario 3.

4.1.2. Sensitivity for min and max electricity prices

The basic analysis of all heat pumps was done for average electricity prices in the EU. Additional assessments were also done for minimum and maximum EU electricity prices to see the sensitivity of the obtained results. Reducing the energy price moves the extremum of the TAC trendline of Scenario 1 into the higher compressor pressure (Figure 6a) but the minimum of the calculation remains at the same point for a condensation pressure of 1,050 kPa. The increase in energy price moves the min TAC point to a condensation pressure of 900 kPa and overall trends become increasing (Figure 6b). The changes in total cost share of Case Study 1 for min and max energy prices are shown in Figure 7.

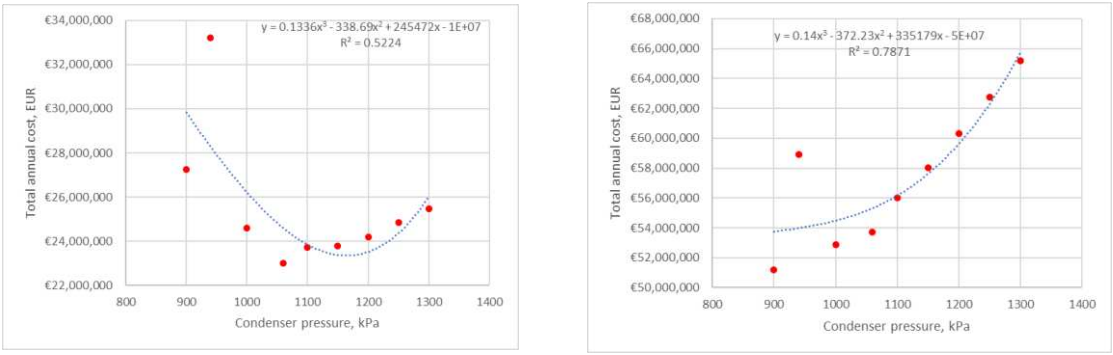

(**a**) (**b**)

Figure 6. Total annual cost correlation of Heat Pump 1 for scenario 1: (**a**) min electricity price; (**b**) max electricity price.

 doi:10.20944/preprints202402.0217.v1

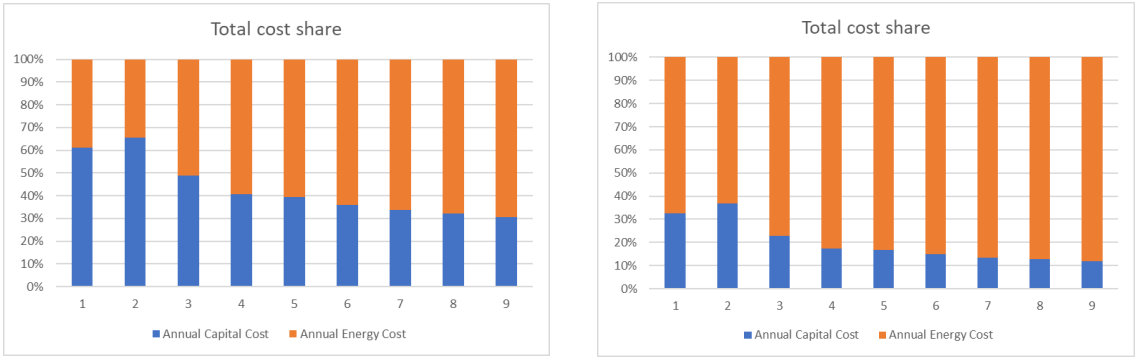

(**a**) (**b**)

Figure 7. Total cost distribution of Heat Pump 1 for scenario 1: (**a**) min electricity price; (**b**) max electricity price.

Changes in energy prices do not affect seriously the TAC cost trend of HP 1 in Scenario 2 which is demonstrated in Figure 8, minimum value remains for condenser pressure 480 kPa. The share of energy and capital cost is shown in Figure 9.

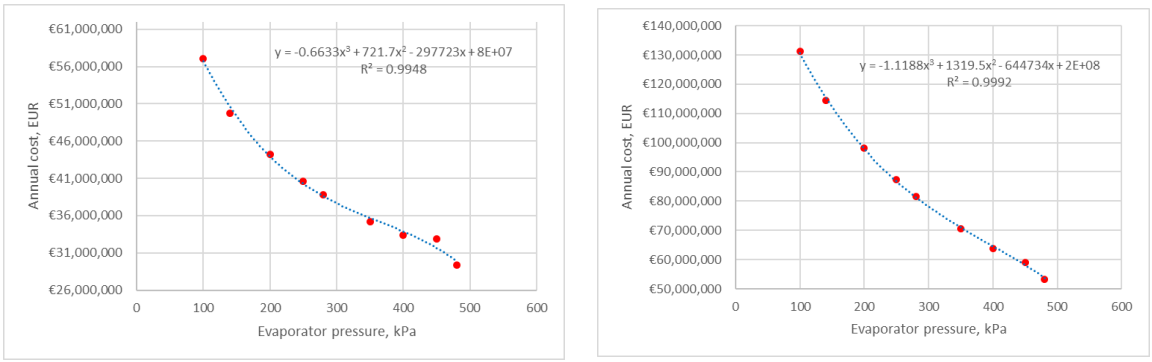

(**a**) (**b**)

Figure 8. Total annual cost correlation of Heat Pump 1 for scenario 2: (**a**) min electricity price; (**b**) max electricity price.

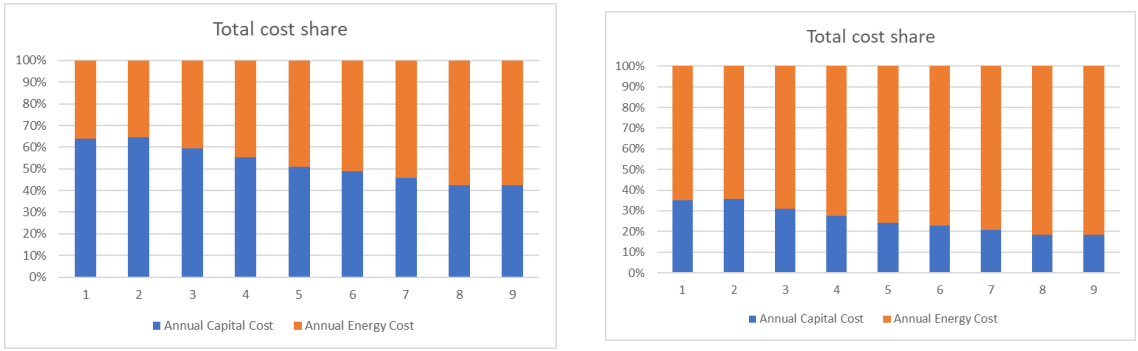

(**a**) (**b**)

Figure 9. Total cost distribution of Heat Pump 1 for scenario 2: (**a**) min electricity price; (**b**) max electricity price.

The reduction of energy price affects the results of Scenario 3 of the HP 1 and extremum appears for calculation point 3 with an evaporation pressure of 400 kPa and condensation pressure of 1,000 kPa (Figure 10a). This case can be seen in Figure 11a, and the share of energy cost is 60 %, which less

 doi:10.20944/preprints202402.0217.v1

than for min TAC with average electricity prices. The increase in energy prices does not influence the nature of the trend line.

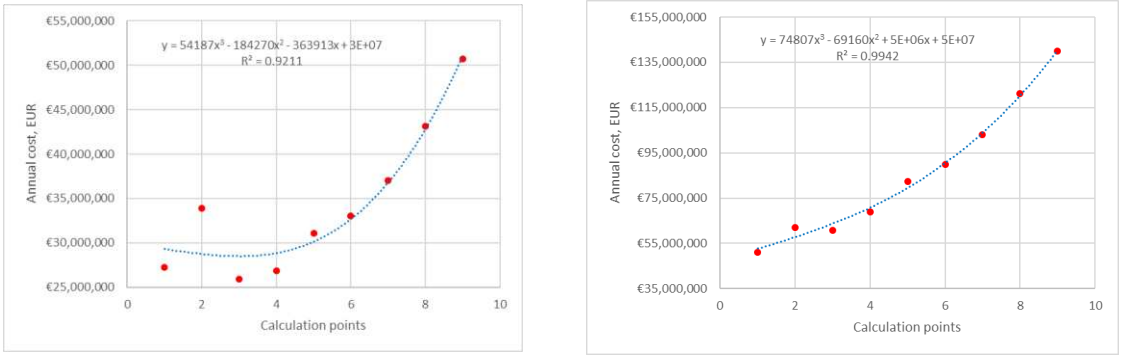

(**a**) (**b**)

Figure 10. Total annual cost correlation of Heat Pump 1 for scenario 3: (**a**) min electricity price; (**b**) max electricity price.

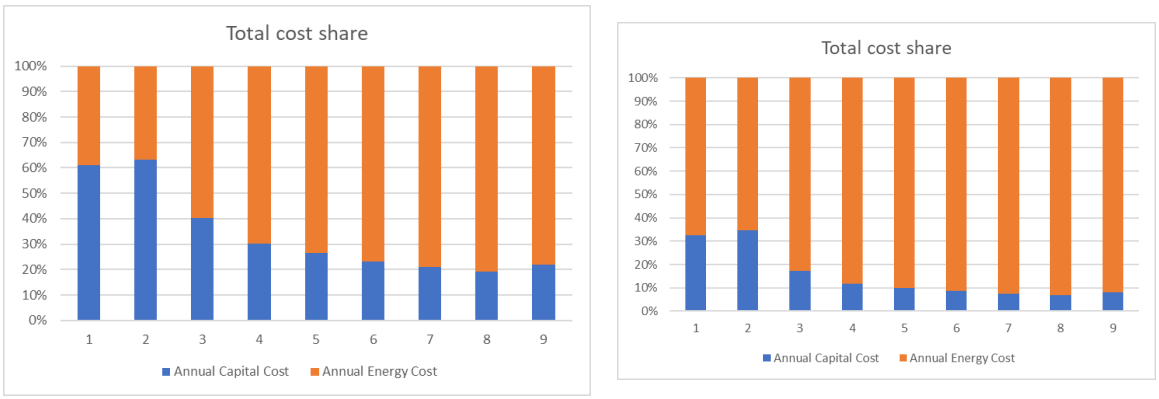

(**a**) (**b**)

Figure 11. Total cost distribution of Heat Pump 1 for scenario 3: (**a**) min electricity price; (**b**) max electricity price.

4.2. Heat pump 2.

4.2.1. Average electricity price

The correlation of the TAC for HP 2 is more complicated than for HP 1. Figure 12 demonstrates the min TAC for Scenario 1 (Figure 12a) and Scenario 3 (Figure 12c) but Scenario 3 has more apparent extremum. The TAC in Scenario 2 (Figure 12b) has an increasing trend while decreasing evaporation pressure. The minimum TAC is found for Scenario 1, and it is 8.56 M€ for a condensation pressure of 1,050 kPa. The minimum TAC of Scenario 3 is 8.77 M€, which is very close to first one and it is found for condensation pressure 950 kPa and evaporation pressure of 390 kPa.

Preprints.org (www.preprints.org) | NOT PEER-REVIEWED | Posted: 5 February 2024 doi:10.20944/preprints202402.0217.v1

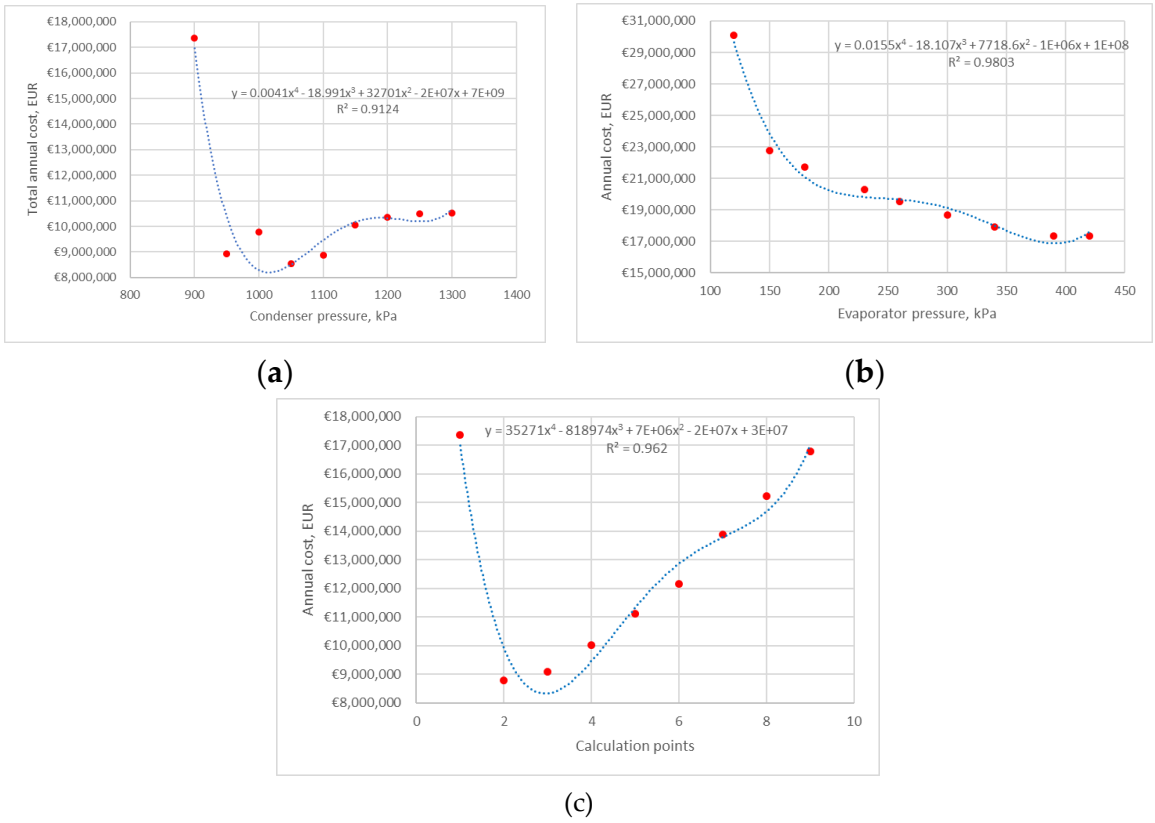

Figure 12. Total annual cost correlation of Heat Pump 2 for average electricity price: (**a**) scenario 1; (**b**) scenario 2; (**c**) scenario 3.

The distribution of capital cost shows the highest share of the condenser cost for Scenario 2 (Figure 13b) and the increasing share of compressor cost for Scenario 3 (Figure 13c). The distribution of equipment cost for Scenario 1 is not linear (Figure 13a). The condenser cost is decreasing while the compressor and evaporator cost is fluctuating.

The share of energy and capital cost for Scenario 2 is shown in Figure 14. It should be noted that the share of energy cost, for the case studies with extremum of TAC, is 68 % for Scenario 1 (point 4) and 62 % for Scenario 3 (point 2).

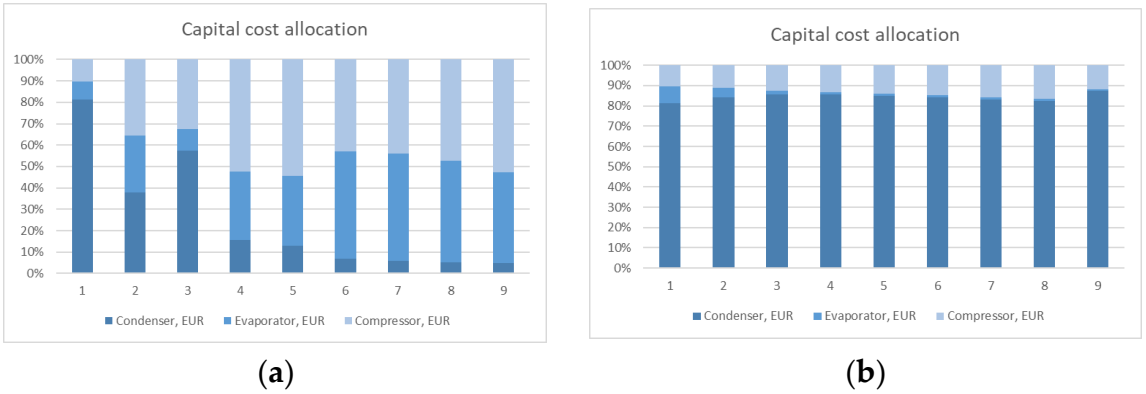

Preprints.org (www.preprints.org) | NOT PEER-REVIEWED | Posted: 5 February 2024 doi:10.20944/preprints202402.0217.v1

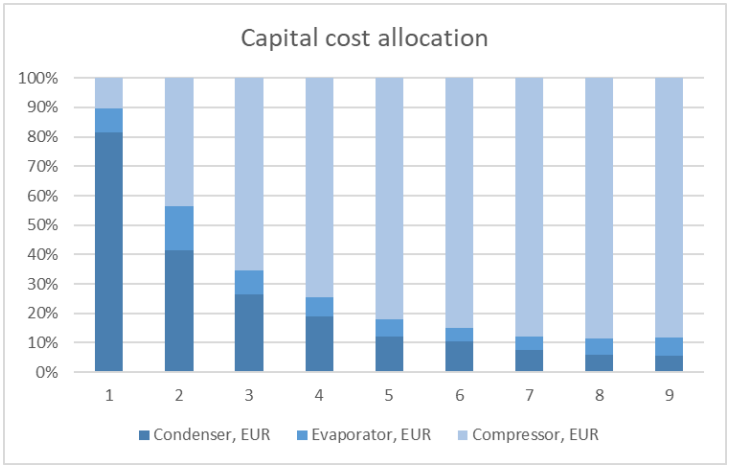

(c)

Figure 13. Capital cost allocation of Heat Pump 2: (**a**) scenario 1; (**b**) scenario 2; (**c**) scenario 3.

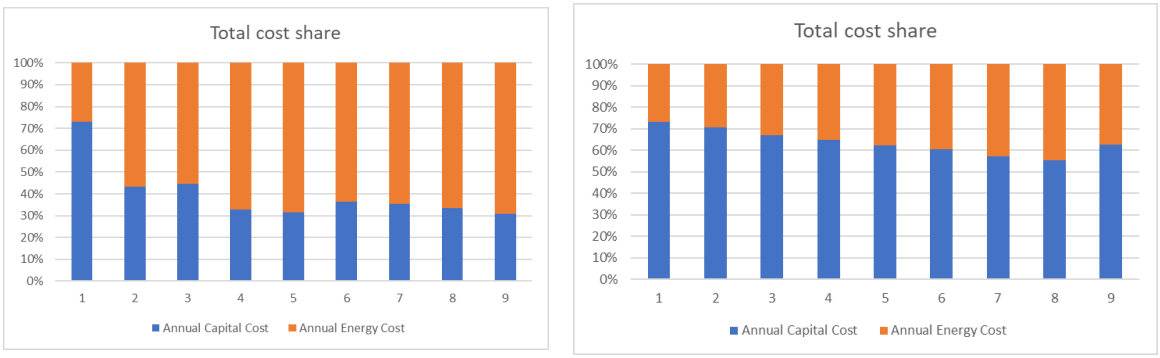

(**a**) (**b**)

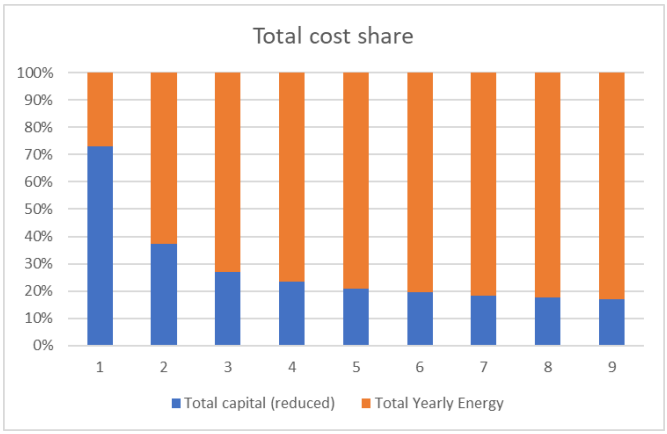

(c)

Figure 14. Total cost distribution of Heat Pump 2 for average electricity price: (**a**) scenario 1; (**b**) scenario 2; (**c**) scenario 3.

4.2.2. Sensitivity for min and max electricity prices

The investigation of the results for Scenario 1 obtained for max EU electricity price demonstrates that minimum TAC is observed for condensation pressure 950 kPa (Figure 15b). The min electricity price does not affect seriously to the results of Scenario 1 and min TAC remains at 1050 kPa (condenser) that is confirmed by the correlation in Figure 15a. The share of the energy cost for the solutions with min TAC of HP 2 is 54 % for min electricity prices and 71 % for max EU electricity prices (Figure 16).

Preprints.org (www.preprints.org) | NOT PEER-REVIEWED | Posted: 5 February 2024 doi:10.20944/preprints202402.0217.v1

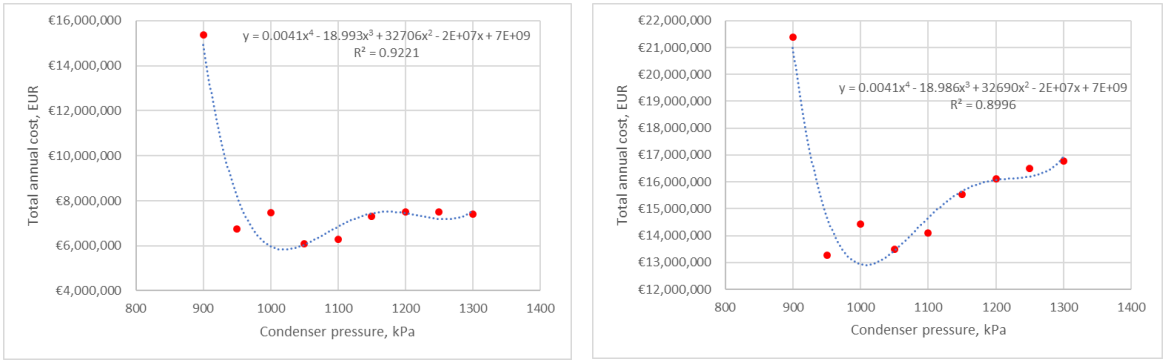

(**a**) (**b**)

Figure 15. Total annual cost correlation of Heat Pump 2 for scenario 1: (**a**) min electricity price; (**b**) max electricity price.

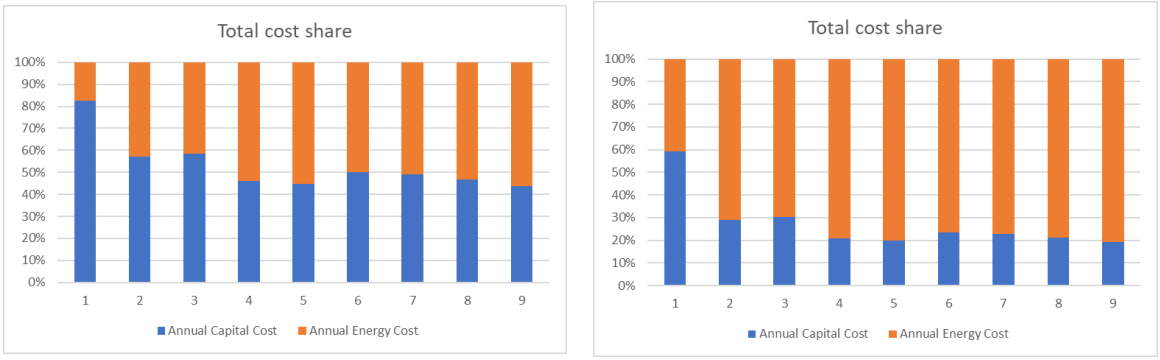

(**a**) (**b**)

Figure 16. Total cost distribution of Heat Pump 2 for scenario 1: (**a**) min electricity price; (**b**) max electricity price.

The results of Scenario 2 for max and min EU electricity prices are shown in Figures 17 and 18. Min energy prices move the min TAC point to evaporation pressure 380 kPa but the extremum is not strongly marked. Max energy prices do not affect seriously to TAC trendline.

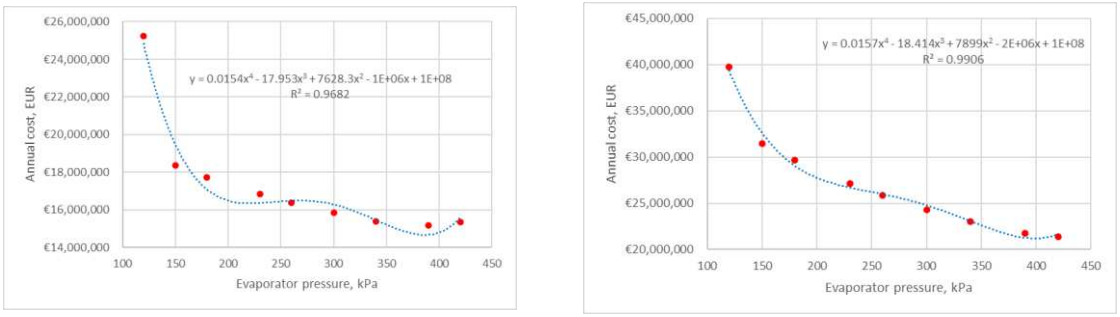

(**a**) (**b**)

Figure 17. Total annual cost correlation of Heat Pump 2 for scenario 2: (**a**) min electricity price; (**b**) max electricity price.

Preprints.org (www.preprints.org) | NOT PEER-REVIEWED | Posted: 5 February 2024 doi:10.20944/preprints202402.0217.v1

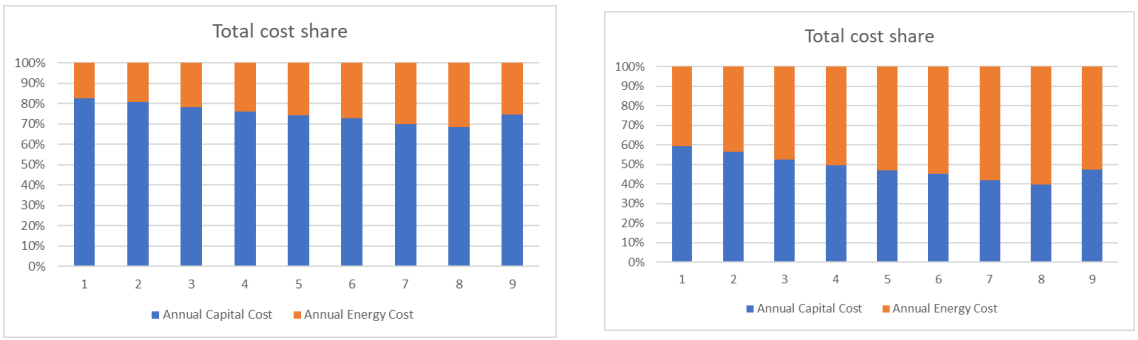

(**a**) (**b**)

Figure 18. Total cost distribution of Heat Pump 2 for scenario 2: (**a**) min electricity price; (**b**) max electricity price.

The results of Scenario 3 for min energy prices shifts the min TAC to point 3 (condensation pressure 1,000 kPa, evaporation pressure 340 kPa) (Figure 19a). Max energy prices remain the min TAC at the same process condition (Figure19b). The share of the energy cost is 61 % for min electricity price and 76 % for max electricity price (Figure 20).

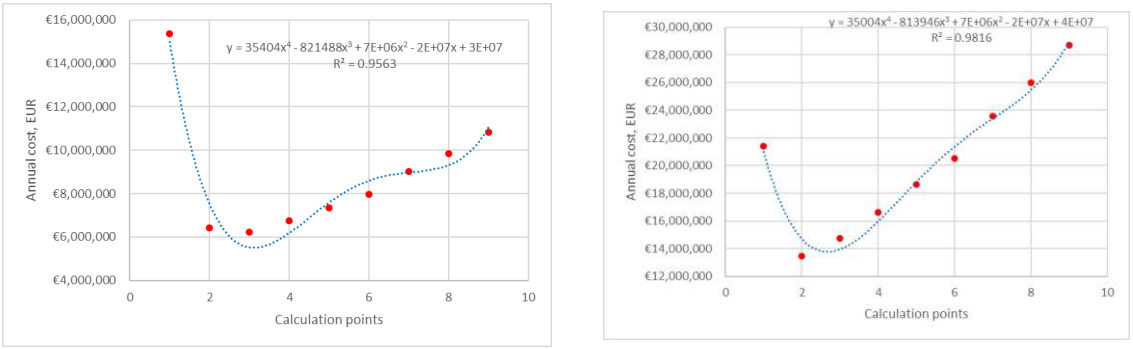

(**a**) (**b**)

Figure 19. Total annual cost correlation of Heat Pump 2 for scenario 3: (**a**) min electricity price; (**b**) max electricity price.

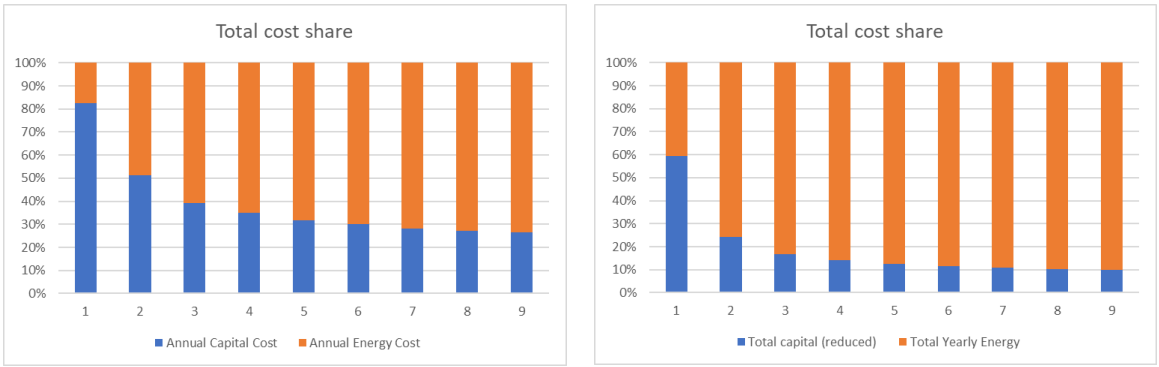

(**a**) (**b**)

Figure 20. Total cost distribution of Heat Pump 2 for scenario 3: (**a**) min electricity price; (**b**) max electricity price.

 doi:10.20944/preprints202402.0217.v1

4.3. Heat pump 3.

4.3.1. Average electricity price

The investigation of the TAC results for all scenarios of HP 3 shows that the correlation is monotonous and increases while condensation pressure increases or evaporation pressure decreases. It is well-illustrated in Figure 21. The same situation is for capital cost distribution where the share of the compressor increase for condenser pressure increase and evaporator pressure reduction (Figure 22). High share of energy cost in TAC is for all three scenarios and this value is more than 80 % (Figure 23). It can be justified by low COP of HP 3 in comparison to two previous ones.

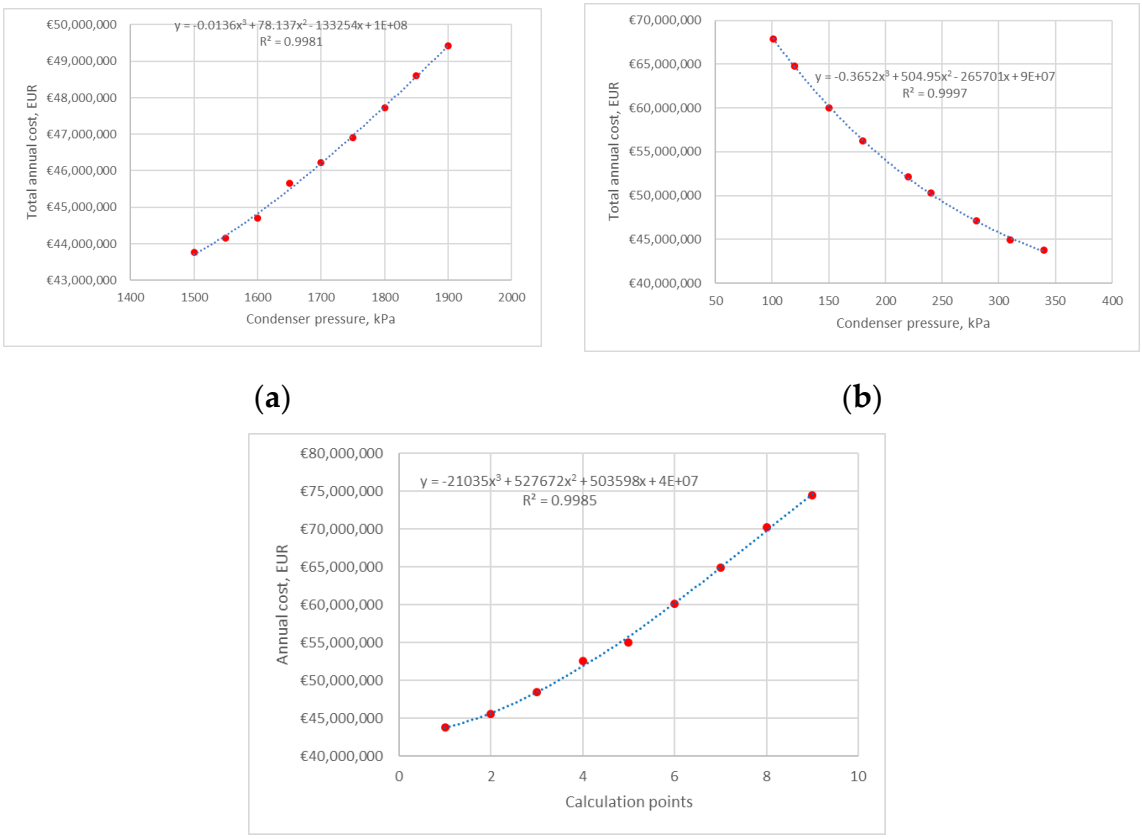

Figure 21. Total annual cost correlation of Heat Pump 3 for average electricity price: (**a**) scenario 1; (**b**) scenario 2; (**c**) scenario 3.

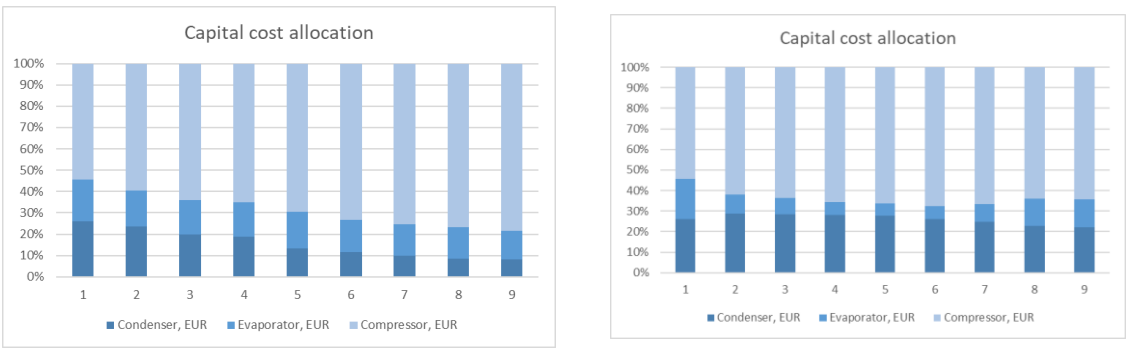

 doi:10.20944/preprints202402.0217.v1

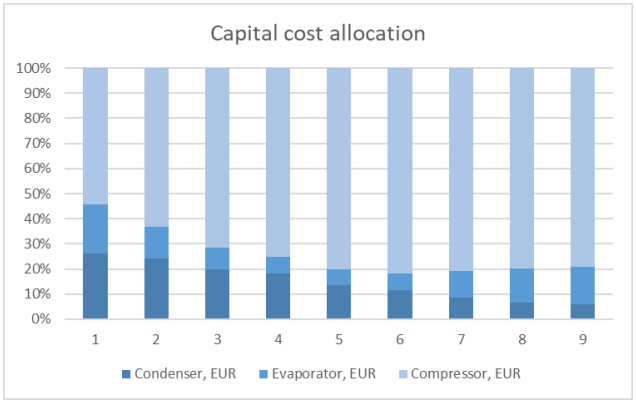

(c)

Figure 22. Capital cost allocation of Heat Pump 3: (**a**) scenario 1; (**b**) scenario 2; (**c**) scenario 3.

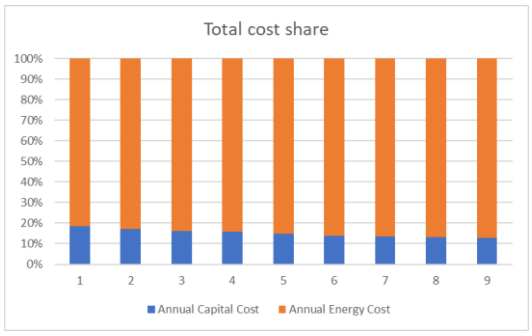

(**a**)

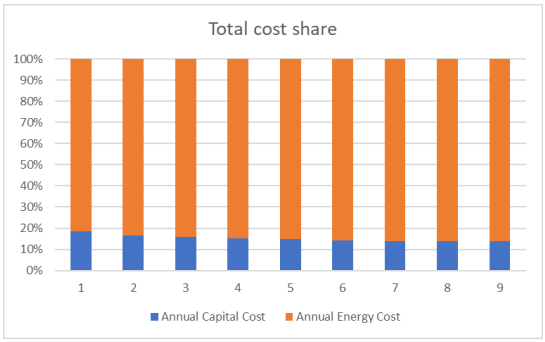

(**b**)

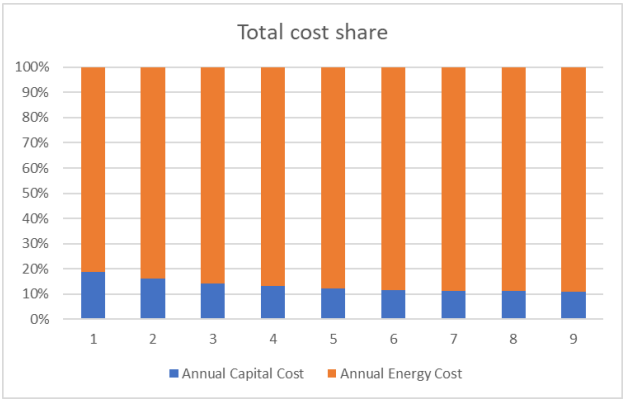

(c)

Figure 23. Total cost distribution of Heat Pump 3 for average electricity price: (**a**) scenario 1; (**b**) scenario 2; (**c**) scenario 3.

4.3.2. Sensitivity for min and max electricity prices

The investigation of the results for min and max electricity prices does not change the overall picture and just changes the share of electricity prices in overall TAC distribution (Figures 24–28). The use of HP 3 is recommended for operation conditions defined from the targeting by the GCC.

 doi:10.20944/preprints202402.0217.v1

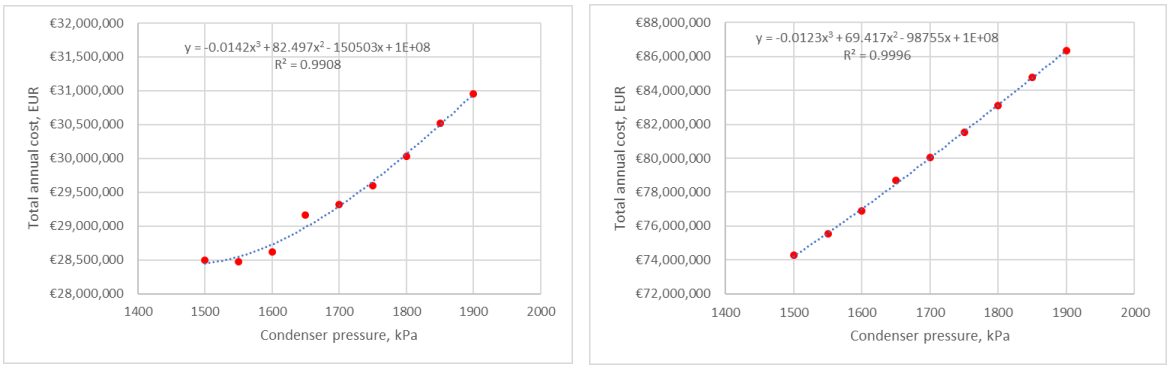

(**a**) (**b**)

Figure 24. Total annual cost correlation of Heat Pump 3 for scenario 1: (**a**) min electricity price; (**b**) max electricity price.

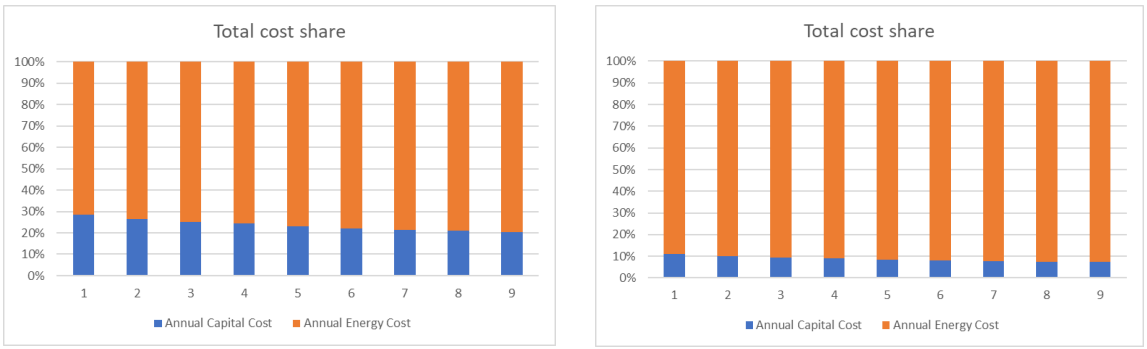

(**a**) (**b**)

Figure 25. Total cost distribution of Heat Pump 3 for scenario 1: (**a**) min electricity price; (**b**) max electricity price.

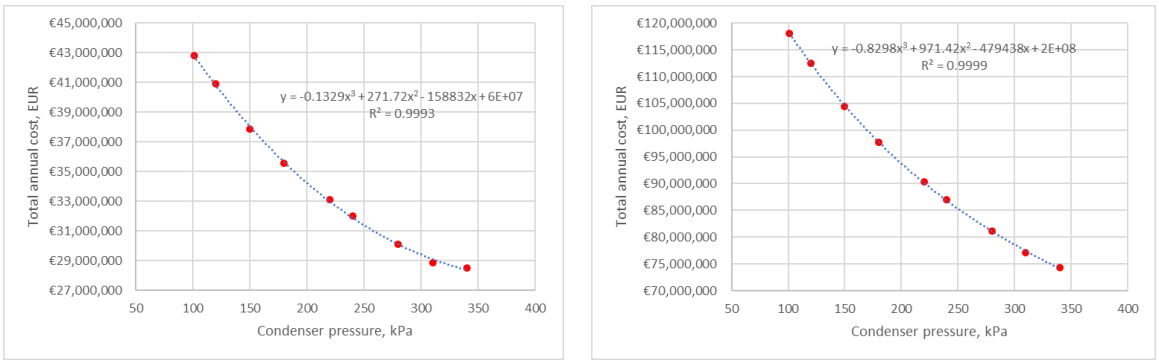

(**a**) (**b**)

Figure 26. Total annual cost correlation of Heat Pump 3 for scenario 2: (**a**) min electricity price; (**b**) max electricity price.

Preprints.org (www.preprints.org) | NOT PEER-REVIEWED | Posted: 5 February 2024 doi:10.20944/preprints202402.0217.v1

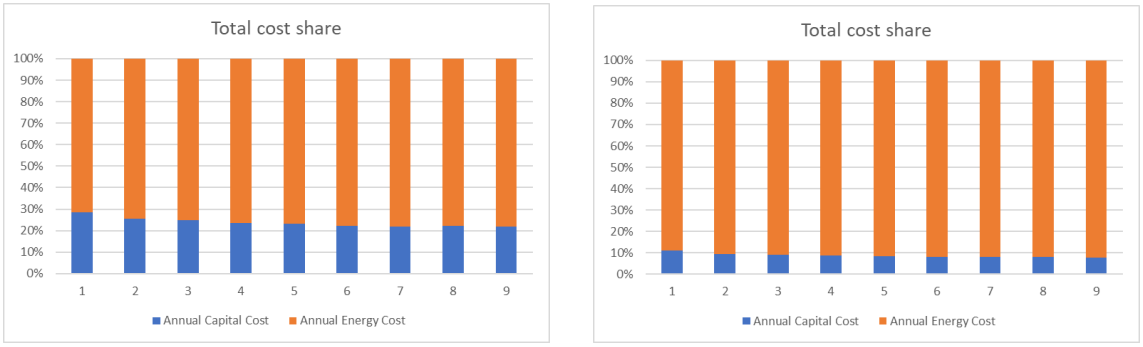

(**a**) (**b**)

Figure 27. Total cost distribution of Heat Pump 3 for scenario 2: (**a**) min electricity price; (**b**) max electricity price.

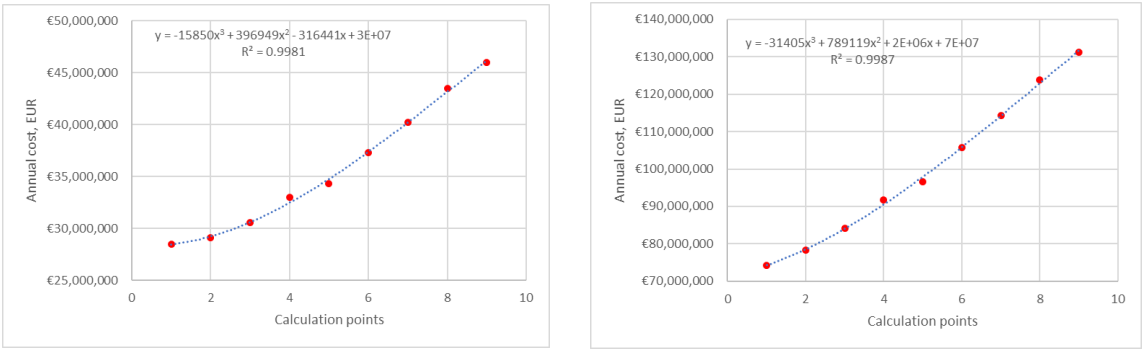

(**a**) (**b**)

Figure 28. Total annual cost correlation of Heat Pump 3 for scenario 3: (**a**) min electricity price; (**b**) max electricity price.

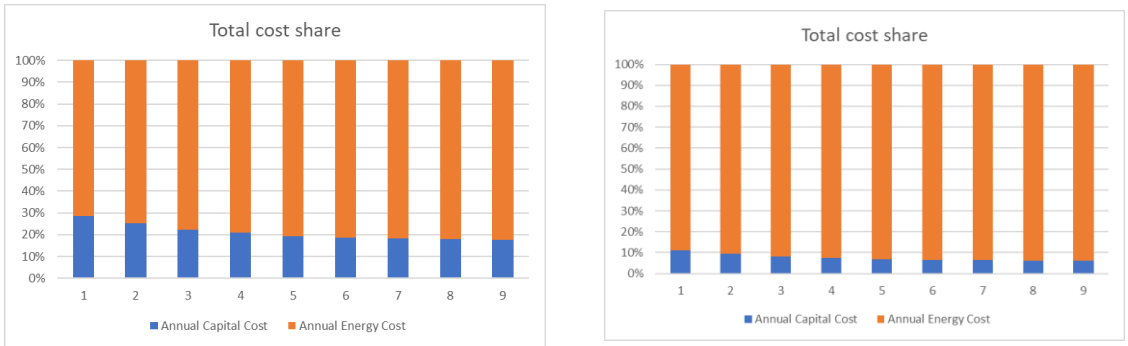

(**a**) (**b**)

Figure 28. Total cost distribution of Heat Pump 3 for scenario 3: (**a**) min electricity price; (**b**) max electricity price.

4.4. Impact of the results.

The obtained results of HP integration into the specific process of polymer plant demonstrated that energy targets obtained from GCC were not always the best solution, especially, an economic one. It is very important when applying heat pumps of high capacity on an industrial scale, the results should be impressive for potential investors and plant owners. Table 7 demonstrates the results of HP calculation for a gas fractioning unit of a polymer plant proposed by a modified targeting approach (optimised). These results are compared with the ones obtained by traditional targeting with the use of the GCC. HP 3 can be applied with its initial operation mode and targets defined by

 doi:10.20944/preprints202402.0217.v1

GCC. HP 1 and HP 2 can be adjusted by selection of the evaporator and condenser temperature to reduce the overall cost. In both cases, the condensation pressure should be changed and TAC reduction is 6 % for HP 1 and 50 % for HP 2.

However, the energy cost and electricity consumption are higher than defined for the base case. This issue is important when electrifying the energy system to the grid and applying renewable energies. On the one hand, we have a more economically viable solution for heat pump applications, and, on another hand, there is more electricity is required from the grid. This issue should be additionally investigated in terms of economic aspects of grid extension driven by renewable energies. It can be also used for appropriate planning of energy needs in future energy systems.

Table 7. Comparison of the results of heat pump application.

	HP-1		**HP-2**		**HP-3**	
	Targeting (Base case)	Optimised	Targeting (Base case)	Optimised	Targeting (Base case)	Optimised
Evaporator						
Inlet temperature, °C	57.65	57.65	52.80	52.80	45.44	45.44
Outlet temperature, °C	58.00	58.00	52.37	52.37	44.95	44.95
Heat duty, kW	95,888	92,825	19,703	19,092	62,185	62,185
LMTD	7.32	7.32	2.66	3.09	5.12	5.12
Heat transfer area, m^2	24,029	22,921	6,199	5,672	9,998	9,998
Condenser						
Inlet temperature, °C	97.07	107.75	99.30	109.33	138.12	138.12
Outlet temperature, °C	82.29	89.57	82.29	89.14	106.04	106.04
Heat duty, kW	106,692	106,697	22,430	22,430	82,863	82,863
LMTD	7.46	17.17	8.08	17.41	16.45	16.45
Heat transfer area, m^2	67,957	17,229	72,576	2,648	13,782	13,782
Compressor						
Inlet pressure, kPa	480	480	420	420	340	340
Outlet pressure, kPa	900	1,060	900	1,050	1,500	1,500
Power, kW	10,804	13,877	2,727	3,338	20,678	20,678
COP	9.87	7.69	8.22	6.72	4.01	4.01
Economic indicators						
Annual capital cost, k€	16,619	9,353	12,673	2,811	8,150	8,150
Energy cost, k€/y[1]	18,611	23,901	4,696	5,747	35,608	35,608
Total annual cost, k€/y	35,231	33,255	17,369	8,559	43,758	43,758

6. Conclusions

This paper presented the results of heat pumps integration into the industrial process of the polymer plant. Electrification of the thermal utility of distillation columns of the gas fractioning unit was done by three heat pumps utilising 212 MW of waste heat. The approach for reduction of the cost for heat pump application is proposed that is based on the detailed simulation of heat pump heat

[1] *Defined for average energy prices*

 doi:10.20944/preprints202402.0217.v1

exchangers and overall operation conditions. The trade-off between capital cost and energy cost was investigated and optimised operation conditions of heat pumps were selected. The results were compared with the ones obtained by energy targeting with the Grand Composite Curves.

The total annual costs of Heat Pump 1 and Heat Pump 2 were reduced by 6 % and 50 % respectively, in comparison to the configuration of heat pumps targeted by Grand Composite Curves. But it requires an increase of electricity consumption of 22 % and 18 % for Heat Pump 1 and Heat Pump 2 and additional thermal utility for cooling increased by 3 % for both heat pumps. The total annual cost for the application of both heat pumps is reduced by 21.5 M€, which may be impressive for the investors when integrating heat pumps into the specific polymer plant. Heat Pump 3 can be applied with the same operating conditions as defined by the Grand Composite Curve.

The total saving of thermal hot utility by all three heat pumps is 212 MW, which was initially covered by steam generated by fossil fuel burning. It corresponds to a saving of 1.41 $ktCO_2/y$ if considering the carbon intensity of fossil fuel of 0.163 tCO_2/kWh.

This approach can update the targeting procedure that is used for THE pinch-based approach to reduce the total annual cost when integrating heat pumps within the industrial sectors. The utility pinches can be also characterised by a higher temperature approach that simplifies the design of condensers and reboilers.

Supplementary Materials: There is no supplementary material to this article.

Author Contributions: Conceptualization, S.B.; methodology, S.B.; software, M.I., S.B; validation, M.I., G.K.; formal analysis, M.I.; investigation, S.B., M.I.; resources, M.I., G.K..; data curation, M.I.; writing—original draft preparation, M.I., S.B.; writing—review and editing, C.B.; visualization, M.I., S.B.; supervision, S.B.; project administration, S.B.; funding acquisition, G.K., S.B. All authors have read and agreed to the published version of the manuscript.

Funding: This research was funded by the European Commission, under Project 101119793 — LIFE22-CET-SET_HEAT.

Data Availability Statement: Data is available upon request.

Conflicts of Interest: The authors declare no conflict of interest.

Nomenclature

A	Heat transfer area (m^2)
ACC	Annual capital cost (€/y)
c_e	Electricity prices (€/kWh)
$CAPEX_{Evap}$	Evaporator capital cost (€)
$CAPEX_{Comp}$	Compressor capital cost (€)
$CAPEX_{Cond}$	Condenser capital cost (€)
COP_{HP}	Coefficient of performance (n/d)
d_0	Outside diameter of tube (m)
EC	Annual energy cost (€/y)
$f(t)$	Correction factor for materials of construction (n/d)
$f(p)$	Correction factor for design pressure (n/d)
$f(m)$	Correction factor for materials of construction (n/d)
FIR	Fractional interest rate per year (%)
Ft	Correction factor of heat transfer (n/d)
g	Gravitational constant (9.81 $m \cdot s^{-2}$)
h_C	Condensing film coefficient ($W \cdot m^{-2} \cdot K^{-1}$)
h_j^{In}	Enthalpy of the inlet stream ($kJ\ kg^{-1}$)
h_j^{Out}	Enthalpy of the outlet stream ($kJ\ kg^{-1}$)

 doi:10.20944/preprints202402.0217.v1

h_{NB}	Nucleate boiling coefficient (W·m^{-2}·K^{-1})
J	Number of process streams, (n/d)
k_L	Thermal conductivity of the liquid (W·m^{-1}·K^{-1})
$Lang$	Lang factor (n/d)
M_j^{In}	Mass flow of the inlet stream (kg h^{-1})
M_j^{Out}	Mass flow of the oulet stream (kg h^{-1})
M_{losses}	Losses of mass flows (kg h^{-1})
NY	Bank loan period (y)
P	Operating pressure (kPa)
P_C	Liquid critical pressure (kPa)
Q	Heat duty (W)
q	Heat flux (W·m^{-2})
Q_{HP}	Heat absorbed by heat pump at low temperature (W)
Q_{losses}	Energy losses (W)
TAC	Total annual cost (€/y)
T_{inC}	Inlet temperature of the cold stream (°C)
T_{inH}	Inlet temperature of the hot stream (°C)
T_{outC}	Outlet temperature of the cold stream (°C)
T_{outH}	Outlet temperature of the hot stream (°C)
U	Heat trasfer coefficient (W·m^{-2}·K^{-1})
W_i	Power (W)
ΔH_{VAP}	Latent heat (J·kg−1)
ΔT_{LM}	Logarithmic temperature difference (°C)
ΔT	Temperature difference across the condensate film (°C)
μ_L	Viscosity of the liquid (kg·m^{-1}·s^{-1})
ρ_L	Density of the liquid (kg·m^{-3})

References

1. Barkaoui, A.-E.; Boldyryev, S.; Duic, N.; Krajacic, G.; Guzović, Z. Appropriate Integration of Geothermal Energy Sources by Pinch Approach: Case Study of Croatia. *Applied Energy* **2016**, *184*, 1343–1349, doi:10.1016/j.apenergy.2016.04.112.
2. Mészáros, I.; Fonyó, Z. Design Strategy for Heat Pump Assisted Distillation System. *Journal of Heat Recovery Systems* **1986**, *6*, 469–476, doi:10.1016/0198-7593(86)90039-1.
3. van de Bor, D.M.; Infante Ferreira, C.A.; Kiss, A.A. Low Grade Waste Heat Recovery Using Heat Pumps and Power Cycles. *Energy* **2015**, *89*, 864–873, doi:10.1016/j.energy.2015.06.030.
4. Yuan, G.; Chu, K.H. Heat Pump Drying of Industrial Wastewater Sludge. *Water Practice and Technology* **2020**, *15*, 404–415, doi:10.2166/wpt.2020.029.
5. Tveit, T.-M. Application of an Industrial Heat Pump for Steam Generation Using District Heating as a Heat Source. **2017**.
6. Byrne, P.S.; Carton, J.G.; Corcoran, B. Investigating the Suitability of a Heat Pump Water-Heater as a Method to Reduce Agricultural Emissions in Dairy Farms. *Sustainability* **2021**, *13*, 5736, doi:10.3390/su13105736.
7. Hermanucz, P.; Geczi, G.; Barotfi, I. Energy Efficient Solution in the Brewing Process Using a Dual-Source Heat Pump. *Therm sci* **2022**, *26*, 2311–2319, doi:10.2298/TSCI210901026H.
8. Anifantis, A.; Colantoni, A.; Pascuzzi, S.; Santoro, F. Photovoltaic and Hydrogen Plant Integrated with a Gas Heat Pump for Greenhouse Heating: A Mathematical Study. *Sustainability* **2018**, *10*, 378, doi:10.3390/su10020378.
9. Nemś, A.; Nemś, M.; Świder, K. Analysis of the Possibilities of Using a Heat Pump for Greenhouse Heating in Polish Climatic Conditions—A Case Study. *Sustainability* **2018**, *10*, 3483, doi:10.3390/su10103483.

10. Słyś, D.; Pochwat, K.; Czarniecki, D. An Analysis of Waste Heat Recovery from Wastewater on Livestock and Agriculture Farms. *Resources* **2020**, *9*, 3, doi:10.3390/resources9010003.
11. Babak, T.; Duić, N.; Khavin, G.; Boldyryev, S.; Krajačić, G. Possibility of Heat Pump Use in Hot Water Supply Systems. *[Journal of Sustainable Development of Energy, Water and Environment Systems]* **2016**, *[4]*, [203]-[215].
12. Ünal, F.; Akan, A.E.; DemiR, B.; Yaman, K. 4E Analysis of an Underfloor Heating System Integrated to the Geothermal Heat Pump for Greenhouse Heating. *Turkish Journal of Agriculture and Forestry* **2022**, *46*, 762–780, doi:10.55730/1300-011X.3040.
13. Chiriboga, G.; Capelo, S.; Bunces, P.; Guzmán, C.; Cepeda, J.; Gordillo, G.; Montesdeoca, D.E.; Carvajal C, G. Harnessing of Geothermal Energy for a Greenhouse in Ecuador Employing a Heat Pump: Design, Construction, and Feasibility Assessment. *Heliyon* **2021**, *7*, e08608, doi:10.1016/j.heliyon.2021.e08608.
14. Zhang, H.; Liu, Y.; Liu, X.; Duan, C. Energy and Exergy Analysis of a New Cogeneration System Based on an Organic Rankine Cycle and Absorption Heat Pump in the Coal-Fired Power Plant. *Energy Conversion and Management* **2020**, *223*, 113293, doi:10.1016/j.enconman.2020.113293.
15. Cao, X.-Q.; Yang, W.-W.; Zhou, F.; He, Y.-L. Performance Analysis of Different High-Temperature Heat Pump Systems for Low-Grade Waste Heat Recovery. *Applied Thermal Engineering* **2014**, *71*, 291–300, doi:10.1016/j.applthermaleng.2014.06.049.
16. Zhang, H.; Dong, Y.; Lai, Y.; Zhang, H.; Zhang, X. Waste Heat Recovery from Coal-Fired Boiler Flue Gas: Performance Optimization of a New Open Absorption Heat Pump. *Applied Thermal Engineering* **2021**, *183*, 116111, doi:10.1016/j.applthermaleng.2020.116111.
17. Su, W.; Ma, D.; Lu, Z.; Jiang, W.; Wang, F.; Xiaosong, Z. A Novel Absorption-Based Enclosed Heat Pump Dryer with Combining Liquid Desiccant Dehumidification and Mechanical Vapor Recompression: Case Study and Performance Evaluation. *Case Studies in Thermal Engineering* **2022**, *35*, 102091, doi:10.1016/j.csite.2022.102091.
18. Jokiel, M.; Bantle, M.; Kopp, C.; Halvorsen Verpe, E. Modelica-Based Modelling of Heat Pump-Assisted Apple Drying for Varied Drying Temperatures and Bypass Ratios. *Thermal Science and Engineering Progress* **2020**, *19*, 100575, doi:10.1016/j.tsep.2020.100575.
19. Waheed, M.A.; Oni, A.O.; Adejuyigbe, S.B.; Adewumi, B.A.; Fadare, D.A. Performance Enhancement of Vapor Recompression Heat Pump. *Applied Energy* **2014**, *114*, 69–79, doi:10.1016/j.apenergy.2013.09.024.
20. Liu, Y.; Zhai, J.; Li, L.; Sun, L.; Zhai, C. Heat Pump Assisted Reactive and Azeotropic Distillations in Dividing Wall Columns. *Chemical Engineering and Processing: Process Intensification* **2015**, *95*, 289–301, doi:10.1016/j.cep.2015.07.001.
21. Long, N.V.D.; Minh, L.Q.; Pham, T.N.; Bahadori, A.; Lee, M. Novel Retrofit Designs Using a Modified Coordinate Descent Methodology for Improving Energy Efficiency of Natural Gas Liquid Fractionation Process. *Journal of Natural Gas Science and Engineering* **2016**, *33*, 458–468, doi:10.1016/j.jngse.2016.05.038.
22. Long, N.V.D.; Han, T.H.; Lee, D.Y.; Park, S.Y.; Hwang, B.B.; Lee, M. Enhancement of a R-410A Reclamation Process Using Various Heat-Pump-Assisted Distillation Configurations. *Energies* **2019**, *12*, 3776, doi:10.3390/en12193776.
23. Zhu, Z.; Qi, H.; Shen, Y.; Qiu, X.; Zhang, H.; Qi, J.; Yang, J.; Wang, L.; Wang, Y.; Ma, Y.; et al. Energy-Saving Investigation of Organic Material Recovery from Wastewater via Thermal Coupling Extractive Distillation Combined with Heat Pump Based on Thermoeconomic and Environmental Analysis. *Process Safety and Environmental Protection* **2021**, *146*, 441–450, doi:10.1016/j.psep.2020.09.014.
24. Šulgan, B.; Labovský, J.; Variny, M.; Labovská, Z. Multi-Objective Assessment of Heat Pump-Assisted Ethyl Acetate Production. *Processes* **2021**, *9*, 1380, doi:10.3390/pr9081380.
25. Boldyryev, S.; Kuznetsov, M.; Ryabova, I.; Krajačić, G.; Kaldybaeva, B. Assessment of Renewable Energy Use in Natural Gas Liquid Processing by Improved Process Integration with Heat Pumps. *e-Prime - Advances in Electrical Engineering, Electronics and Energy* **2023**, *5*, 100246, doi:10.1016/j.prime.2023.100246.
26. Schlosser Florian; Arpagaus Cordin; Walmsley Timothy Gordon Heat Pump Integration by Pinch Analysis for Industrial Applications: A Review. *Chemical Engineering Transactions* **2019**, *76*, 7–12, doi:10.3303/CET1976002.
27. Kim, Y.; Lim, J.; Shim, J.Y.; Hong, S.; Lee, H.; Cho, H. Optimization of Heat Exchanger Network via Pinch Analysis in Heat Pump-Assisted Textile Industry Wastewater Heat Recovery System. *Energies* **2022**, *15*, 3090, doi:10.3390/en15093090.
28. Timothy G. Walmsley; Jiri Jaromir Klemes; Michael R.W. Walmsley; Martin J. Atkins; Petar S. Varbanov Innovative Hybrid Heat Pump for Dryer Process Integration. *Chemical Engineering Transactions* **2017**, *57*, 1039–1044, doi:10.3303/CET1757174.
29. Gai Limei; Varbanov Petar Sabev; Walmsley Timothy Gordon; Klemes Jiri Jaromir Process Integration Using a Joule Cycle Heat Pump. *Chemical Engineering Transactions* **2019**, *76*, 415–420, doi:10.3303/CET1976070.
30. Lincoln, B.J.; Kong, L.; Pineda, A.M.; Walmsley, T.G. Process Integration and Electrification for Efficient Milk Evaporation Systems. *Energy* **2022**, *258*, 124885, doi:10.1016/j.energy.2022.124885.

31. Klinac, E.; Carson, J.K.; Hoang, D.; Chen, Q.; Cleland, D.J.; Walmsley, T.G. Multi-Level Process Integration of Heat Pumps in Meat Processing. *Energies* **2023**, *16*, 3424, doi:10.3390/en16083424.
32. Ulyev L.; Kapustenko P.; Vasilyev M.; Boldyryev S. Total Site Integration for Coke Oven Plant. *Chemical Engineering Transactions* **2013**, *35*, 235–240, doi:10.3303/CET1335039.
33. Hegely, L.; Lang, P. Reduction of the Energy Demand of a Second-Generation Bioethanol Plant by Heat Integration and Vapour Recompression between Different Columns. *Energy* **2020**, *208*, 118443, doi:10.1016/j.energy.2020.118443.
34. Cox, J.; Belding, S.; Lowder, T. Application of a Novel Heat Pump Model for Estimating Economic Viability and Barriers of Heat Pumps in Dairy Applications in the United States. *Applied Energy* **2022**, *310*, 118499, doi:10.1016/j.apenergy.2021.118499.
35. Lu, Z.; Yao, Y.; Liu, G.; Ma, W.; Gong, Y. Thermodynamic and Economic Analysis of a High Temperature Cascade Heat Pump System for Steam Generation. *Processes* **2022**, *10*, 1862, doi:10.3390/pr10091862.
36. Martínez-Rodríguez, G.; Díaz-de-León, C.; Fuentes-Silva, A.L.; Baltazar, J.-C.; García-Gutiérrez, R. Detailed Thermo-Economic Assessment of a Heat Pump for Industrial Applications. *Energies* **2023**, *16*, 2784, doi:10.3390/en16062784.
37. Chen, T.; Kyung Kwon, O. Experimental Analyses of Moderately High-Temperature Heat Pump Systems with R245fa and R1233zd(E). *Energy Engineering* **2022**, *119*, 2231–2242, doi:10.32604/ee.2022.021289.
38. Zühlsdorf, B.; Bühler, F.; Mancini, R.; Cignitti, S. High Temperature Heat Pump Integration Using Zeotropic Working Fluids for Spray Drying Facilities. **2017**.
39. Gómez-Hernández, J.; Grimes, R.; Briongos, J.V.; Marugán-Cruz, C.; Santana, D. Carbon Dioxide and Acetone Mixtures as Refrigerants for Industry Heat Pumps to Supply Temperature in the Range 150–220 oC. *Energy* **2023**, *269*, 126821, doi:10.1016/j.energy.2023.126821.
40. Gudjonsdottir, V.; Infante Ferreira, C.A. Technical and Economic Analysis of Wet Compression–Resorption Heat Pumps. *International Journal of Refrigeration* **2020**, *117*, 140–149, doi:10.1016/j.ijrefrig.2020.05.010.
41. 15 Thermodynamic and Economic Analysis of the Integration of High-Temperature Heat Pumps.Pdf.
42. Wolf, M.; Detzlhofer, T.; Proll, T. A Comparative Study of Industrial Heat Supply Based on Second-Law Analysis and Operating Costs. *Therm sci* **2018**, *22*, 2203–2213, doi:10.2298/TSCI171228217W.
43. Zuberi, M.J.S.; Hasanbeigi, A.; Morrow, W. Techno-Economic Evaluation of Industrial Heat Pump Applications in US Pulp and Paper, Textile, and Automotive Industries. *Energy Efficiency* **2023**, *16*, 19, doi:10.1007/s12053-023-10089-6.
44. Wu, X.; Xing, Z.; He, Z.; Wang, X.; Chen, W. Performance Evaluation of a Capacity-Regulated High Temperature Heat Pump for Waste Heat Recovery in Dyeing Industry. *Applied Thermal Engineering* **2016**, *93*, 1193–1201, doi:10.1016/j.applthermaleng.2015.10.075.
45. Gangar, N.; Macchietto, S.; Markides, C.N. Recovery and Utilization of Low-Grade Waste Heat in the Oil-Refining Industry Using Heat Engines and Heat Pumps: An International Technoeconomic Comparison. *Energies* **2020**, *13*, 2560, doi:10.3390/en13102560.
46. Yang, L.; Ren, Y.; Wang, Z.; Hang, Z.; Luo, Y. Simulation and Economic Research of Circulating Cooling Water Waste Heat and Water Resource Recovery System. *Energies* **2021**, *14*, 2496, doi:10.3390/en14092496.
47. Lee, J.; Son, Y.; Lee, K.; Won, W. Economic Analysis and Environmental Impact Assessment of Heat Pump-Assisted Distillation in a Gas Fractionation Unit. *Energies* **2019**, *12*, 852, doi:10.3390/en12050852.
48. Hou, J.; Mao, C.; Xu, Y. Thermoeconomic Multiobjective Optimization of Tobacco Drying Heat Pump Recovering Waste Heat from Monocrystal Silicon Furnace Based on SVR ANN Model in Southwest China. *Energy Science & Engineering* **2023**, ese3.1458, doi:10.1002/ese3.1458.
49. Aspen HYSYS | Process Simulation Software | AspenTech Available online: https://www.aspentech.com/en/products/engineering/aspen-hysys (accessed on 31 January 2024).
50. Kern's Process Heat Transfer, 2nd Edition | Wiley Available online: https://www.wiley.com/en-us/Kern%27s+Process+Heat+Transfer%2C+2nd+Edition-p-9781119364825 (accessed on 29 January 2024).
51. Hewitt, G.F. *Handbook of Heat Exchanger Design*; Begell House, 1992; ISBN 978-1-56700-000-9.
52. Electricity Price Statistics - Statistics Explained Available online: https://ec.europa.eu/eurostat/statistics-explained/index.php?title=Electricity_price_statistics (accessed on 31 January 2024).
53. Aspen Exchanger Design and Rating (EDR) | AspenTech Available online: https://www.aspentech.com/en/products/engineering/aspen-exchanger-design-and-rating (accessed on 31 January 2024).